

Search for supersymmetry with a compressed mass spectrum in the vector boson fusion topology with 1-lepton and 0-lepton final states in proton-proton collisions at $\sqrt{s} = 13$ TeV



The CMS collaboration

E-mail: cms-publication-committee-chair@cern.ch

ABSTRACT: A search for supersymmetric particles produced in the vector boson fusion topology in proton-proton collisions is presented. The search targets final states with one or zero leptons, large missing transverse momentum, and two jets with a large separation in rapidity. The data sample corresponds to an integrated luminosity of 35.9 fb^{-1} of proton-proton collisions at $\sqrt{s} = 13$ TeV collected in 2016 with the CMS detector at the LHC. The observed dijet invariant mass and lepton-neutrino transverse mass spectra are found to be consistent with the standard model predictions. Upper limits are set on the cross sections for chargino ($\tilde{\chi}_1^\pm$) and neutralino ($\tilde{\chi}_2^0$) production with two associated jets. For a compressed mass spectrum scenario in which the $\tilde{\chi}_1^\pm$ and $\tilde{\chi}_2^0$ decays proceed via a light slepton and the mass difference between the lightest neutralino $\tilde{\chi}_1^0$ and the mass-degenerate particles $\tilde{\chi}_1^\pm$ and $\tilde{\chi}_2^0$ is 1 (30) GeV, the most stringent lower limit to date of 112 (215) GeV is set on the mass of these latter two particles.

KEYWORDS: Hadron-Hadron scattering (experiments), Supersymmetry

ARXIV EPRINT: [1905.13059](https://arxiv.org/abs/1905.13059)

Contents

1	Introduction	1
2	The CMS detector	4
3	Event reconstruction and particle identification	4
4	Signal and background samples	6
5	Event selection	7
6	Background estimation	9
7	Systematic uncertainties	13
8	Results and interpretation	15
9	Summary	18
	The CMS collaboration	25

1 Introduction

Supersymmetry (SUSY) [1–7] is a theory that can simultaneously describe the particle nature of dark matter (DM) and solve the gauge hierarchy problem of the standard model (SM). However, for all of its attractive features, there is as yet no direct evidence to support this theory. The masses of the strongly produced gluinos (\tilde{g}) as well as the squarks (\tilde{q}) of the first and second generations have been excluded below approximately 2 TeV in certain simplified model scenarios [8–13]. On the other hand, the values of the masses of the weakly produced charginos ($\tilde{\chi}_i^\pm$) and neutralinos ($\tilde{\chi}_i^0$) are less constrained at the CERN LHC where these particles have much smaller production cross sections. The chargino-neutralino sector of SUSY plays an important role in establishing a connection between SUSY models and DM. The lightest neutralino $\tilde{\chi}_1^0$, as the lightest supersymmetric particle (LSP), is the canonical DM candidate in R -parity conserving SUSY extensions of the SM [14].

A common strategy to search for charginos and neutralinos is through Drell-Yan (DY) production processes of order α_{EW}^2 (electroweak coupling squared) involving virtual W and Z bosons (W^*/Z^*), $q\bar{q}' \rightarrow W^* \rightarrow \tilde{\chi}_i^\pm \tilde{\chi}_j^0$, followed by their decay to final states with one or more charged leptons (ℓ) and missing transverse momentum ($p_{\text{T}}^{\text{miss}}$). These processes can include, for example, $\tilde{\chi}_1^\pm \tilde{\chi}_2^0$ pair production followed by $\tilde{\chi}_1^\pm \rightarrow \ell^\pm \nu_\ell \tilde{\chi}_1^0$ and $\tilde{\chi}_2^0 \rightarrow \ell^\pm \ell^\mp \tilde{\chi}_1^0$ via virtual SM bosons or a light slepton $\tilde{\ell}$, where $\tilde{\chi}_1^\pm$ ($\tilde{\chi}_2^0$) is the lightest (next-to-lightest) chargino (neutralino), and where the LSP $\tilde{\chi}_1^0$ is presumed to escape without detection

leading to significant missing momentum. However, these searches are experimentally difficult in cases where the mass of the LSP is only slightly less than the masses of other charginos and neutralinos, making these so-called compressed spectrum scenarios important search targets using new techniques. While the exclusion limits in refs. [15–17] can be as stringent as $m_{\tilde{\chi}_1^\pm} < 650$ GeV for a massless $\tilde{\chi}_1^0$, they weaken to only approximately 100 GeV for $\Delta m \equiv m_{\tilde{\chi}_1^\pm} - m_{\tilde{\chi}_1^0} = 2$ GeV, assuming decays of the $\tilde{\chi}_1^\pm$ and $\tilde{\chi}_2^0$ to leptonic final states proceed through the mediation of virtual W and Z bosons [18, 19]. As the mass difference between SUSY particles decreases, the momenta available to the co-produced SM particles are small, resulting in “soft” decay products having low transverse momentum (p_T). Therefore, the traditional searches using DY processes suffer in the compressed spectrum scenarios since the SM particles used for discrimination become more difficult to reconstruct as their momenta decrease. In contrast, chargino and neutralino production via vector boson fusion (VBF) processes of order α_{EW}^4 are very useful in tackling these interesting compressed SUSY scenarios [20]. In VBF processes, electroweak SUSY particles are pair-produced in association with two high- p_T oppositely-directed jets close to the beam axis (forward), resulting in a large dijet invariant mass (m_{jj}). The use of two high- p_T VBF jets in the event topology effectively suppresses the SM background while, simultaneously, creating a recoil effect that facilitates both the detection of p_T^{miss} in the event and the identification of the soft decay products in compressed-spectrum scenarios because of their natural kinematic boost [21, 22]. Figure 1 shows the Feynman diagrams for two of the possible VBF production processes: chargino-neutralino and chargino-chargino production.

The CMS collaboration reported the first results of a SUSY search using the VBF dijet topology for charginos and neutralinos in the minimal supersymmetric standard model (MSSM), using a data sample corresponding to an integrated luminosity of 19.7 fb^{-1} of proton-proton collision data at $\sqrt{s} = 8$ TeV [23]. That analysis considered SUSY models with light staus ($\tilde{\tau}$) leading to leptonic decay modes of the charginos and neutralinos (e.g., $\tilde{\chi}_2^0 \rightarrow \tau^\pm \tilde{\tau}^\mp \rightarrow \tau^- \tau^+ \tilde{\chi}_1^0$). In the presence of a light slepton, it is likely that $\tilde{\chi}_1^\pm$ decays to $\ell^\pm \nu_\ell \tilde{\chi}_1^0$ and $\tilde{\chi}_2^0$ decays to $\ell^+ \ell^- \tilde{\chi}_1^0$. Thus, charginos and neutralinos were probed using final states with two leptons and two additional jets consistent with the VBF topology. In the compressed mass spectrum scenario, where the mass difference between the $\tilde{\chi}_1^0$ and $\tilde{\chi}_2^0/\tilde{\chi}_1^\pm$ particles was taken to be 50 GeV, $\tilde{\chi}_2^0$ and $\tilde{\chi}_1^\pm$ masses below 170 GeV were excluded.

In this paper, a search is presented for the electroweak production of SUSY particles in the VBF topology using data collected in 2016 with the CMS detector and corresponding to an integrated luminosity of 35.9 fb^{-1} of proton-proton collisions at a center-of-mass energy of $\sqrt{s} = 13$ TeV. Besides the two oppositely directed forward jets (j) that define the VBF configuration, the search requires the presence of zero or one soft lepton and large p_T^{miss} . The events are classified into two categories based on the lepton content, $0\ell jj$ and $1\ell jj$, with the latter having three different final states: $e jj$, μjj , and $\tau_h jj$, where τ_h denotes a hadronically decaying τ lepton. The $0\ell jj$ final state (also referred to as the “invisible” channel) provides the best sensitivity to the $\Delta m < 10$ GeV scenarios, where the leptons from the $\tilde{\chi}_2^0/\tilde{\chi}_1^\pm$ decays are “lost”, either because their momenta are too low to reconstruct or because they fail to satisfy the identification requirements. The soft single-lepton channels were not

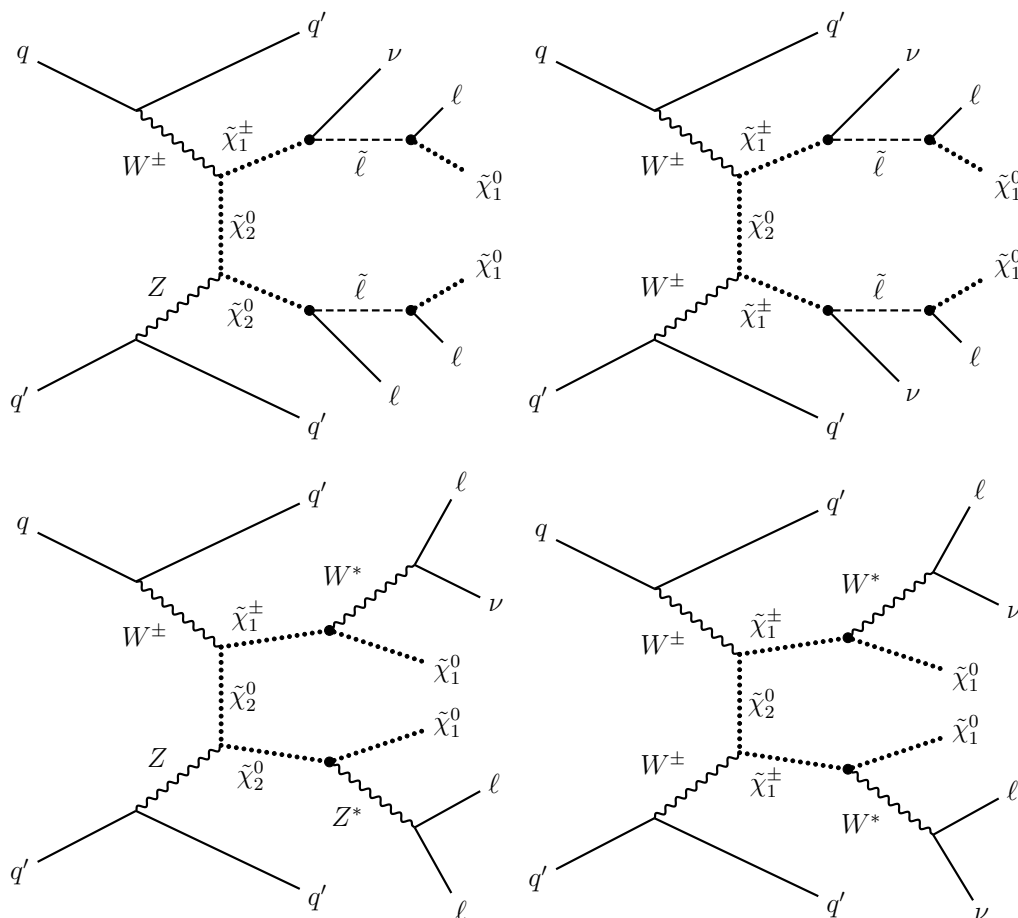


Figure 1. Representative Feynman diagrams of (left) chargino-neutralino and (right) chargino-chargino pair production through vector boson fusion, followed by their decays to leptons and the LSP $\tilde{\chi}_1^0$ via a light slepton (top row) or a W^*/Z^* (bottom row). Although these representative diagrams show multiple leptons in the final state, the compressed mass spectra scenarios of interest result in low- p_T leptons, making it unlikely to reconstruct and identify more than one lepton.

utilized in the 8 TeV search and thus this analysis extends the previous search performed only in the two-lepton final state. The dijet invariant mass distribution m_{jj} is the sensitive variable used to discriminate possible SUSY signal from background in the $0\ell jj$ channel, while the transverse mass m_T between the lepton and p_T^{miss} is used in the $1\ell jj$ channels.

The backgrounds are evaluated using data wherever possible. The general strategy is to define control regions, each dominated by a different background process and with negligible contamination from signal events, through modification of the nominal selection requirements. These control regions are used to measure the m_{jj} and m_T shapes and probabilities for background events to satisfy the VBF selection requirements. If the background contribution from a particular process is expected to be small or if the above approach is not feasible, the m_{jj} and m_T shapes are taken from simulation. In these cases, scale factors, defined as the ratio of efficiencies measured in data and simulation, are used to normalize the predicted rates to the data.

The paper is organized as follows. The CMS detector is described in section 2. The reconstruction of electrons, muons, τ_h leptons, jets, and p_T^{miss} is presented in section 3. The simulated SUSY signal and background samples are discussed in section 4, followed by the description of the event selection in section 5 and the background estimation in section 6. Systematic uncertainties are summarized in section 7, and the results are presented in section 8. Section 9 contains a summary of the paper.

2 The CMS detector

The central feature of the CMS apparatus is a superconducting solenoid of 6 m internal diameter, providing a magnetic field of 3.8 T. Located within the solenoid volume are silicon pixel and strip detectors, a lead tungstate electromagnetic calorimeter (ECAL), and a brass and scintillator hadron calorimeter (HCAL). Muons are measured in gas-ionization detectors embedded in the steel flux-return yoke outside the solenoid. Extensive forward calorimetry complements the barrel and endcap detectors by covering the pseudorapidity range $3.0 < |\eta| < 5.2$.

The inner silicon tracker measures charged tracks with $|\eta| < 2.5$ and provides an impact parameter resolution of approximately $15 \mu\text{m}$ and a transverse momentum resolution of about 1.5% for 100 GeV charged particles. Collision events of interest are selected using a two-tiered trigger system. The first level trigger (L1), composed of custom hardware processors, selects events at a rate of around 100 kHz. The second level trigger, based on an array of microprocessors running a version of the full event reconstruction software optimized for fast processing, reduces the event rate to around 1 kHz before data storage. A detailed description of the CMS detector, along with a definition of the coordinate system and relevant kinematic variables, can be found in ref. [24].

3 Event reconstruction and particle identification

The particle-flow (PF) algorithm is used to reconstruct the jets and p_T^{miss} used in this analysis [25]. The PF technique combines information from different subdetectors to produce a mutually-exclusive collection of particles (namely muons, electrons, photons, charged hadrons, and neutral hadrons) that are used as input for the jet clustering algorithms. The missing transverse momentum vector \vec{p}_T^{miss} is defined as the negative vector sum of the momenta of all reconstructed PF candidates in an event, projected on the plane perpendicular to the beam axis. The magnitude of \vec{p}_T^{miss} is p_T^{miss} [26]. The production of undetected particles such as SM neutrinos and the SUSY $\tilde{\chi}_1^0$ is inferred by the measured p_T^{miss} . The reconstructed vertex with the largest value of summed physics-object p_T^2 is taken to be the primary pp interaction vertex. The physics objects are the jets, clustered using the jet finding algorithm [27, 28] with the tracks assigned to the vertex as inputs, and the associated missing transverse momentum, taken as the negative vector sum of the p_T of those jets.

Jets are clustered using the FASTJET anti- k_T algorithm [27, 28], with a distance parameter of 0.4. Only jets that satisfy the identification criteria designed to reject particles from

multiple proton-proton interactions (pileup) and anomalous behavior in the calorimeters are considered in this analysis [29]. The jet energy scale and resolution are calibrated through correction factors that depend on the p_T and η of the jet [30]. Jets with $p_T > 60$ GeV have a reconstruction-plus-identification efficiency of approximately 99%, while 90–95% of pileup jets are rejected [31]. Jets originating from the hadronization of bottom quarks (b quark jets) are identified using the combined secondary vertex (CSV) algorithm [32], which exploits observables related to the long lifetime of B hadrons. For jets with $p_T > 20$ GeV and $|\eta| < 2.4$, the b tagging algorithm is operated at a working point such that the probability of correctly identifying a b quark jet is approximately 60%, while the probability of misidentifying a jet generated from a light-flavor quark or gluon as a b quark jet is approximately 1% [32].

Muons are reconstructed using the inner silicon tracker and muon detectors [33]. Quality requirements based on the minimum number of measurements in the silicon tracker, pixel detector, and muon detectors are applied to suppress backgrounds from decays-in-flight and hadron shower remnants that reach the muon system. Electrons are reconstructed by combining tracks produced by the Gaussian-sum filter algorithm with ECAL clusters [34]. Requirements on the track quality, the shape of the energy deposits in the ECAL, and the compatibility of the measurements from the tracker and the ECAL are imposed to distinguish prompt electrons from charged pions and from electrons produced by photon conversions. The electron and muon reconstruction efficiencies are $>99\%$ for $p_T > 8$ GeV.

The electron and muon candidates are required to satisfy isolation criteria in order to reject non-prompt leptons from the hadronization of quarks and gluons. Relative isolation is defined as the scalar sum of the p_T values of reconstructed charged and neutral particles within a cone of radius $\Delta R \equiv \sqrt{(\Delta\eta)^2 + (\Delta\phi)^2} = 0.4$ (where ϕ is the azimuthal angle in radians) around the lepton-candidate track, divided by the p_T of the lepton candidate. To suppress the effects of pileup, tracks from charged particles not associated with the primary vertex are excluded from the isolation sum, and the contribution to pileup from reconstructed neutral hadrons is subtracted [29]. The contribution from the electron or muon candidate is removed from the sum. The value of the isolation variable is required to be ≤ 0.0821 for electrons and ≤ 0.25 for muons [33, 34].

The total efficiency for the muon identification and isolation requirements is 96% for muons with $p_T > 10$ GeV and $|\eta| < 2.1$. The rate at which pions undergoing $\pi^\pm \rightarrow \mu^\pm \nu_\mu$ decay are misidentified as prompt muons is 10^{-3} for pions with $p_T > 10$ GeV and $|\eta| < 2.1$. The total efficiency for the electron identification and isolation requirements is 85 (80)% for electrons with $p_T > 10$ GeV in the barrel (endcap) region [34]. The jet \rightarrow e misidentification rate is 5×10^{-3} for jets with $p_T > 10$ GeV and $|\eta| < 2.1$ [34].

Hadronic decays of τ leptons are reconstructed and identified using the hadrons-plus-strips algorithm [35], which is designed to optimize the performance of the τ_h reconstruction by considering specific τ_h decay modes. To suppress backgrounds in which light-quark or gluon jets can mimic τ_h decays, a τ_h candidate is required to be spatially isolated from other energy deposits in the event. The isolation variable is calculated using a multivariate

boosted decision tree technique within a cone of radius $\Delta R = 0.5$ around the direction of the τ_h candidate and considering the energy deposits of particles not included in the reconstruction of the τ_h decay mode. Additionally, τ_h candidates are required to be distinguishable from electrons and muons in the event by using dedicated criteria based on the consistency among the measurements in the tracker, calorimeters, and muon detectors. With these requirements, the contribution from electrons and muons being misidentified as genuine τ_h candidates is negligible ($\ll 0.1\%$).

The identification and isolation efficiency at the tight working point used in this analysis is approximately 50% for a τ_h lepton with $p_T > 20$ GeV and $|\eta| < 2.1$, while the probability for a jet to be misidentified as a τ_h is 1–5%, depending on the p_T and η values of the τ_h candidate [35]. Although the tight working point is used to define the τ_{hjj} signal region, a loose working point is used to obtain multijet enriched control samples for estimation of the background rate in the signal region. The identification and isolation efficiency for a τ_h lepton at the loose working point used in this analysis is approximately 60%, while the probability for a jet to be misidentified as a τ_h is about 10%.

The event selection criteria used in each search channel are summarized in section 5.

4 Signal and background samples

The SM background composition depends on the final state of each channel considered in the analysis. The main backgrounds in the four channels considered in the analysis are estimated using data-driven methods. Negligible or minor backgrounds are obtained directly from simulation. For the ejj and μjj channels, the main backgrounds are from $t\bar{t}$ production and W boson production in association with jets (W+jets). Subdominant background sources come from single top quark, diboson (WW, WZ, and ZZ, collectively referred to as VV) and Z+jets production. For the τ_{hjj} channel, the main source of background consists of SM events only containing jets produced via the strong interaction, referred to as quantum chromodynamics (QCD) multijet events, followed by W+jets and $t\bar{t}$ production. In the $0\ell jj$ channel, the main backgrounds are W/Z+jets and QCD multijet events, with a minor contribution from $t\bar{t}$ and diboson production.

The W+jets, $t\bar{t}$, and single top quark processes produce events with genuine leptons, p_T^{miss} , and jets. The Z+jets process contributes to the background composition when one of the leptons is lost as a result of detector acceptance or inefficiencies in the reconstruction and identification algorithms. Although jets in QCD events have a 1–5% probability of being misidentified as a τ_h , the large QCD multijet production cross section results in a substantial contribution of this background to the τ_{hjj} channel.

In the $0\ell jj$ channel, the Z+jets background produces genuine p_T^{miss} when the Z boson decays into neutrinos. The W+jets process also has real p_T^{miss} when the W boson decays leptonically, but it results in a similar $0\ell jj$ final state when the lepton is not observed as a consequence of the detector acceptance or is not properly reconstructed or identified because of inefficiencies in the corresponding algorithms. The QCD multijet events can also have significant p_T^{miss} from mismeasurement of jet energies.

Simulated samples of signal and background events are generated using Monte Carlo (MC) event generators. The signal event samples are generated with the MADGRAPH5_aMC@NLO v2.3.3 generator [36] at leading order (LO) precision, considering pure electroweak pair production of $\tilde{\chi}_1^\pm$ and $\tilde{\chi}_2^0$ gauginos ($\tilde{\chi}_1^\pm\tilde{\chi}_1^\pm$, $\tilde{\chi}_1^\pm\tilde{\chi}_1^\mp$, $\tilde{\chi}_1^\pm\tilde{\chi}_2^0$, and $\tilde{\chi}_2^0\tilde{\chi}_2^0$) with two associated partons. Models with a bino-like $\tilde{\chi}_1^0$ and wino-like $\tilde{\chi}_2^0$ and $\tilde{\chi}_1^\pm$ are considered. The signal events are generated requiring a pseudorapidity gap $|\Delta\eta| > 3.5$ between the two partons, with $p_T > 30$ GeV for each parton. This parton level $|\Delta\eta|$ requirement is verified to provide no bias with respect to the final requirement on the reconstructed dijet pseudorapidity gap. The LO cross sections in this paper are obtained with these parton-level requirements. Note that VBF $\tilde{\chi}_1^\pm\tilde{\chi}_2^0$ production is the dominant process in the models considered, composing about 60% of the total signal cross section, while the VBF $\tilde{\chi}_1^\pm\tilde{\chi}_1^\mp$ process is the second-largest contribution, composing about 30% of the total signal cross section. The VBF $\tilde{\chi}_1^\pm\tilde{\chi}_1^\pm$ and $\tilde{\chi}_2^0\tilde{\chi}_2^0$ processes compose about 10% of the total signal cross section. The $Z/\gamma^*(\rightarrow\ell^+\ell^-)+\text{jets}$, $Z(\rightarrow\nu_\ell\bar{\nu}_\ell)+\text{jets}$, and $W(\rightarrow\ell\nu_\ell)+\text{jets}$ backgrounds are also simulated at LO precision using MADGRAPH5_aMC@NLO, where up to four partons in the final state are included in the matrix element calculation. The background processes involving the production of a single vector boson in association with two jets exclusively through pure electroweak interactions are simulated at LO via MADGRAPH5_aMC@NLO. The interference effect between pure electroweak and mixed electroweak-QCD production of V+jets events has been studied and found to be small [37]. The effect is neglected in our analysis and the sum of these two samples is henceforth referred to as Z+jets. The QCD multijet background is also simulated at LO using MADGRAPH5_aMC@NLO. Single top quark and $t\bar{t}$ processes are generated at next-to-leading order (NLO) using the POWHEG v2.0 generator [38–42]. The leading order PYTHIA v8.212 generator is used to model the diboson processes. The POWHEG and MADGRAPH generators are interfaced with the PYTHIA v8.212 [43] program, which is used to describe the parton shower and the hadronization and fragmentation processes with the CUETP8M1 tune [44]. The NNPDF3.0 LO and NLO [45] parton distribution functions (PDFs) are used in the event generation. Double counting of the partons generated with MADGRAPH5_aMC@NLO and POWHEG interfaced with PYTHIA is removed using the MLM [46] matching scheme. The LO cross sections are used to normalize simulated signal events, while NLO cross sections are used for simulated backgrounds [36, 42, 47, 48].

For both signal and background simulated events, additional pileup interactions are generated with PYTHIA and superimposed on the primary collision process. The simulated events are reweighted to match the pileup distribution observed in data. The background samples are processed with a detailed simulation of the CMS apparatus using the GEANT4 package [49], while the CMS fast simulation package [50] is used to simulate the CMS detector for the signal samples.

5 Event selection

Events are selected using a trigger with a threshold of 120 GeV on both $p_{T,\text{trig}}^{\text{miss}}$ and $H_{T,\text{trig}}^{\text{miss}}$. The variable $p_{T,\text{trig}}^{\text{miss}}$ corresponds to the magnitude of the vector \vec{p}_T sum of all the PF

candidates reconstructed at the trigger level, while $H_{T,\text{trig}}^{\text{miss}}$ is computed as the magnitude of the vector \vec{p}_T sum of all jets with $p_T > 20 \text{ GeV}$ and $|\eta| < 5.0$ reconstructed at the trigger level. The energy fraction attributed to neutral hadrons in these jets is required to be smaller than 0.9. This requirement suppresses anomalous events with jets originating from detector noise. To be able to use the same trigger for selecting events in the muon control samples used for background prediction, muon candidates are not included in the $p_{T,\text{trig}}^{\text{miss}}$ nor $H_{T,\text{trig}}^{\text{miss}}$ computation. The p_T^{miss} threshold defining the search regions is chosen to achieve a trigger efficiency greater than 95%.

While the compressed mass spectrum SUSY models considered in this analysis result in final states with multiple leptons [20, 22], the compressed mass spectra scenarios of interest also result in low- p_T visible decay products, making it difficult to reconstruct and identify multiple leptons. For this reason, events are required to have zero or exactly one well-identified soft lepton. In the μjj channel, an additional lepton veto is applied by rejecting events containing a second muon ($p_T > 8 \text{ GeV}$), an electron ($p_T > 10 \text{ GeV}$), or a τ_h candidate ($p_T > 20 \text{ GeV}$). Similarly, $e jj$ and $\tau_h jj$ channel events are required not to contain another electron, muon, or τ_h candidate. The $0\ell jj$ channel selects events without a well-identified electron, muon, or τ_h candidate. The veto on additional leptons maintains high efficiency for compressed mass spectra scenarios and simultaneously reduces the SM backgrounds. To further suppress QCD multijet background events containing large p_T^{miss} from jet mismeasurements, the minimum azimuthal separation between any jet with $p_T > 30 \text{ GeV}$ and the direction of the missing transverse momentum vector is required to be greater than 0.5 ($|\Delta\phi_{\text{min}}(\vec{p}_T^{\text{miss}}, j)| > 0.5$). Muon, electron, and τ_h candidates must have $8 < p_T < 40 \text{ GeV}$, $10 < p_T < 40 \text{ GeV}$, and $20 < p_T < 40 \text{ GeV}$, respectively. The upper bound on lepton p_T suppresses the $Z \rightarrow \ell\ell$ and $W \rightarrow \ell\nu_\ell$ backgrounds where the average $p_T(\ell)$ is about $m_Z/2$ and $m_W/2$, respectively. The lower bound on $\tau_h p_T$ is larger because of known difficulties reconstructing lower- p_T τ_h candidates, namely that they do not produce a narrow jet in the detector, which makes them difficult to distinguish from quark or gluon jets. All leptons are required to have $|\eta| < 2.1$ in order to select high quality and well-isolated leptons within the tracker acceptance. This requirement is 99% efficient for signal events. Lepton candidates are also required to pass the reconstruction, identification, and isolation criteria described in section 3.

In addition to the 0ℓ or 1ℓ selection, the following requirements are imposed. The event is required to have $p_T^{\text{miss}} > 250 \text{ GeV}$, which largely suppresses the $Z \rightarrow \ell\ell$ and QCD multijet backgrounds. In order to reduce top quark pair contamination, the event is required not to have any jet identified as a b quark jet, following the description in section 3; only jets with $p_T > 30 \text{ GeV}$, $|\eta| < 2.4$, and separated from the leptons by $\Delta R > 0.3$ are considered for b tags. In the 1ℓ channels, a minimum threshold on the transverse mass between the lepton and the p_T^{miss} is imposed to minimize backgrounds with W bosons. It is required that $m_T(\ell, p_T^{\text{miss}}) > 110 \text{ GeV}$, i.e., beyond the Jacobian m_W peak. The lepton- and p_T^{miss} -based requirements described in this paragraph will be referred to as the “central selection.”

The VBF signal topology is characterized by the presence of two jets in the forward direction, in opposite hemispheres, and with large dijet invariant mass [51–58]. On the other hand, the jets in background events are mostly central and have small dijet invariant

masses. Additionally, the outgoing partons in VBF signal processes must carry relatively large p_T since they must have enough energy (and be within the detector acceptance) to produce a pair of heavy SUSY particles (as shown in figure 1). Therefore, the “VBF selection” is imposed by requiring at least two jets with $p_T > 60$ GeV and $|\eta| < 5.0$. In the $1\ell jj$ channels, only jets separated from the leptons by $\Delta R > 0.3$ are considered. All pairs of jet candidates passing the above requirements and having $|\Delta\eta| > 3.8$ and $\eta_1\eta_2 < 0$ are combined to form VBF dijet candidates. In the rare cases ($< 1\%$) where selected events contain more than one dijet candidate satisfying the VBF criteria, the VBF dijet candidate with the largest dijet mass is chosen since it is 97% likely to result in the correct VBF dijet pair for signal events. Selected dijet candidates are required to have $m_{jj} > 1$ TeV.

The signal region (SR) is defined as the events that satisfy the central and VBF selection criteria.

6 Background estimation

The general methodology used for the estimation of background contributions in the SR is similar for all search channels and is based on both simulation and data. Background-enriched control regions (CR) are constructed by applying selections orthogonal to those for the SR. These CRs are used to measure the efficiencies of the VBF and central selections (the probability for a background component to satisfy the VBF and central selection criteria), determine the correction factors to account for these efficiencies, and derive the shapes of the m_T and m_{jj} background distributions in the SR. The correction factors are determined by assessing the level of agreement in the yields between data and simulation. The shapes of distributions are derived directly from the data in the CR, whenever possible, or from the MC simulated samples when correct modeling by simulation is validated in the dedicated CRs. For each final state, the same trigger is used for the CRs as for the corresponding SR.

The production of $t\bar{t}$ events represents the largest background source in the $e jj$ and μjj channels (approximately 57–64% of the total background), and the second largest background source for the $\tau_h jj$ channel (approximately 29% of the total background). In the $0\ell jj$ final state, since the combination of the lepton and b jet vetoes reduces this background to only approximately 5% of the total background rate, its contribution is determined entirely from simulation. The $t\bar{t}$ background yields in the $1\ell jj$ channels are evaluated using the following equation:

$$N_{t\bar{t}}^{\text{pred}} = N_{t\bar{t}}^{\text{MC}} SF_{t\bar{t}}^{\text{CR}}, \tag{6.1}$$

where $N_{t\bar{t}}^{\text{pred}}$ is the predicted $t\bar{t}$ background yield in the SR, $N_{t\bar{t}}^{\text{MC}}$ is the $t\bar{t}$ rate predicted by simulation for the SR selection, and $SF_{t\bar{t}}^{\text{CR}}$ is the data-over-simulation correction factor, given by the ratio of observed data events to the $t\bar{t}$ yield in simulation, measured in a $t\bar{t}$ enriched CR. The numerator in the calculation of each correction factor is estimated by subtracting from data the contribution from other background events different from that under study, and the statistical uncertainty is propagated to the $SF_{t\bar{t}}^{\text{CR}}$ uncertainty.

The event selection criteria used to define the $t\bar{t}$ CR must not bias the correction factor $SF_{t\bar{t}}^{\text{CR}}$. The simulated samples are used to check the closure of this method, ensuring that the lepton kinematics, the composition of the events, and the m_T and m_{jj} shapes are similar between the CRs and the SR. The closure tests demonstrate that the background determination techniques, described in detail below, reproduce the expected background distributions in both rate and shape to within the statistical uncertainties. Various control samples are also utilized to validate the correct determination of the correction factors with the data.

The $t\bar{t}$ CR is obtained with similar selections to the SR, except requiring one jet tagged as a b quark jet. These control samples with 1 b-tagged jet are referred to as CR_e , CR_μ , and CR_{τ_h} . The 1 b-tagged jet requirement significantly increases the $t\bar{t}$ purity of the control samples while still ensuring that those control samples contain the same kinematics and composition of misidentified leptons as the SR. The $t\bar{t}$ purity of the resulting data CR, determined from simulation, depends on the final state, ranging from 67 to 83%. The measured data-over-simulation correction factors $SF_{t\bar{t}}^{\text{CR}}$ are 0.8 ± 0.3 , 0.8 ± 0.2 , and 1.3 ± 0.5 for the ejj , μjj , and $\tau_h jj$ channels, respectively. The quoted uncertainties are based on the statistics in data and the simulated samples. Systematic uncertainties are discussed in section 7. Figure 2 contains the m_T distributions for the $t\bar{t}$ control regions: (upper left) CR_e , (upper right) CR_μ , and (lower left) CR_{τ_h} . The correction factors $SF_{t\bar{t}}^{\text{CR}}$ have been applied to the MC simulation distributions shown in figure 2. The m_T shapes between data and simulation are consistent within statistical uncertainties (the bands in the data over background (BG) ratio distributions represent the statistical uncertainties of the data and simulated samples). Therefore, the $t\bar{t}$ m_T shapes in the SR are taken directly from simulation.

In general, the W+jets and Z+jets backgrounds represent an important contribution in the $0\ell jj$ and $1\ell jj$ channels, and their contributions to the SR are evaluated using two control regions CR1 and CR2 (defined below for each BG component) and using the equation:

$$N_{\text{BG}}^{\text{pred}} = N_{\text{BG}}^{\text{MC}} SF_{\text{BG}}^{\text{CR1}}(\text{central}) SF_{\text{BG}}^{\text{CR2}}(\text{VBF}), \quad (6.2)$$

where $N_{\text{BG}}^{\text{pred}}$ is the predicted BG yield in the SR, $N_{\text{BG}}^{\text{MC}}$ is the rate predicted by simulation (with BG = W+jets and Z+jets) for the SR selection, $SF_{\text{BG}}^{\text{CR1}}(\text{central})$ is the data-over-simulation correction factor for the central selection, given by the ratio of data to the BG simulation in control region CR1, and $SF_{\text{BG}}^{\text{CR2}}(\text{VBF})$ the data-over-simulation correction factor for the efficiency of the VBF selections as determined in another background enriched control sample CR2.

The production of $Z(\rightarrow \nu\bar{\nu})$ +jets is the main SM background to the $0\ell jj$ SR, with a similar signal topology from the neutrino contributions to p_T^{miss} , and is therefore mostly irreducible. The strategy for the $Z(\rightarrow \nu\bar{\nu})$ +jets background estimation is to use simulation to model the p_T^{miss} distribution, and jet and lepton vetoes. The background yields predicted by the MC simulated samples are corrected for observed differences with respect to the data in the CRs, and scaled to the fraction of events passing the VBF selection, derived from data. The modeling of the m_{jj} distribution is checked in the CRs. Two CRs are used to verify the MC simulation, estimate acceptance corrections used to scale the MC simulation

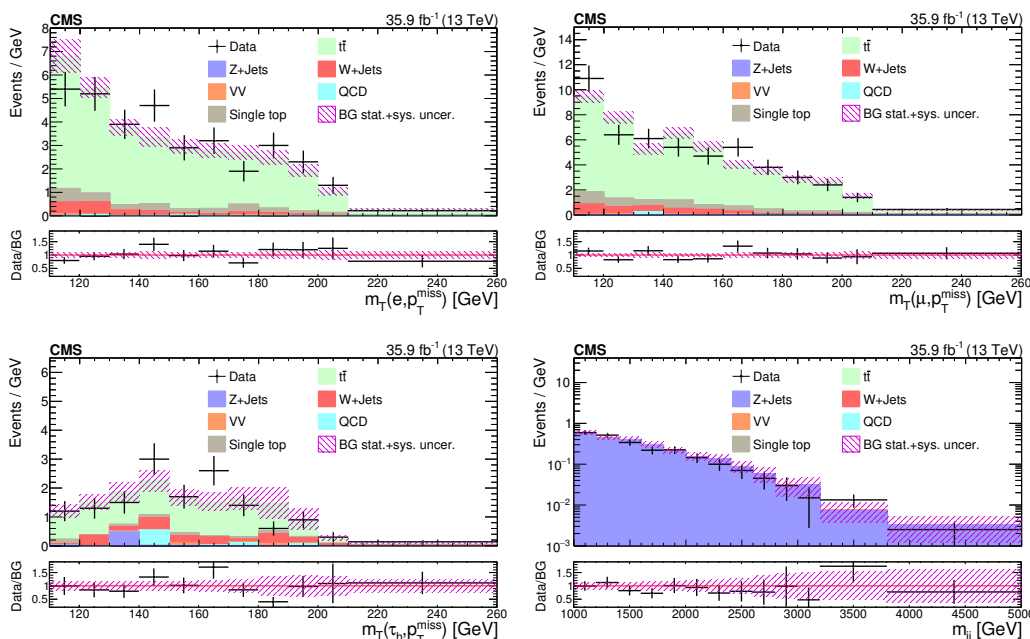


Figure 2. The m_T distributions in the $t\bar{t}$ control regions: (upper left) $CR1_e$, (upper right) $CR1_\mu$, and (lower left) $CR1_{\tau_h}$; (lower right) the m_{jj} distribution for $Z(\rightarrow \nu\bar{\nu})$ +jets $CR2$ of the $0\ell jj$ channel.

yields, and measure the fraction of events passing the VBF selection. The control regions are defined by treating muons as neutrinos in the $Z \rightarrow \mu^+\mu^-$ decay mode. The first control region ($CR1_Z$) is a $Z(\rightarrow \mu^+\mu^-)$ +two jets sample used to validate modeling of geometric and kinematic acceptance of leptons. The invariant mass of the opposite-sign dimuon system must be consistent with the Z -boson mass (60-120 GeV). The two muons are treated as neutrinos, excluding the muon p_T vectors from \vec{p}_T^{miss} , and require $p_T^{\text{miss}} > 250$ GeV together with a veto on b-tagged jets and additional leptons, as in the SR. The measured data-over-simulation correction factor is 0.95 ± 0.02 (stat). Adding the VBF selection defines $CR2_Z$. The Z +jets prediction from simulation in $CR2_Z$ is corrected with the measured data-over-simulation correction factor from $CR1_Z$ to ensure SF_{BG}^{CR2} represents a correction for the efficiency of the VBF selection (correlations between the uncertainties of $CR2_Z$ and $CR1_Z$ are also taken into account). The ratio of $CR2_Z$ to $CR1_Z$ events in the data gives the fraction of $Z(\rightarrow \nu\bar{\nu})$ +jets events passing the VBF topology selection. The measured data-over-simulation correction factor in $CR2_Z$ is 0.92 ± 0.12 (stat). Figure 2 (lower right) shows the m_{jj} distribution in $Z(\rightarrow \nu\bar{\nu})$ +jets $CR2_Z$, which shows agreement between the data and the corrected Z +jets prediction from simulation.

The production of W +jets events presents another important source of background for all the search channels. For the $1\ell jj$ channels, control samples enriched in W +jets events, with about 65% purity according to simulation, are obtained by requiring similar criteria to the SR, except with an inverted VBF selection (failing the VBF selection as defined in section 5). The inverted VBF selection enhances the W +jets background yield by two orders of magnitude, while suppressing the VBF signal contamination to negligible levels. This control region, $CR1_W$, is used to obtain a correction factor for the efficiency of the central selection, SF_{W+jets}^{CR1} (central). This correction factor is determined to be 0.97 ± 0.10 and

1.10 ± 0.10 , for the ejj and μjj channels, respectively. The quoted uncertainties are based on the statistics in data and the simulated samples. For the $\tau_h jj$ channel, it is difficult to obtain a control sample enriched in W +jets events because there is a significant contribution from QCD multijet events. Therefore, the average of the correction factors obtained for the ejj and μjj channels, 1.04 ± 0.13 , is used to scale the W +jets prediction from simulation in the $\tau_h jj$ channel. This approach is justified since the $W(\rightarrow \tau \nu_\tau)$ +jets prediction from simulation is corrected to account for slight differences in the τ_h identification efficiency observed in data. This is further supported by the fact that the modeling of the VBF efficiency at simulation level is uncorrelated with the decay of the W boson. The relatively small difference in mass between W and Z bosons (compared to the energy scale of the SR), which allows the use of a control sample ($CR2_W$) enriched with Z +jets events to measure the VBF selection efficiency for the W +jets background in the $1\ell jj$ channels. This second control sample is obtained by selecting events containing two muons with $p_T > 30$ GeV, treating only one muon as a neutrino to recalculate \vec{p}_T^{miss} , and otherwise similar selections to the SR. Since the efficiency and momentum scale of muons are known at the 1–2% level, any disagreement between data and simulation in this $Z(\rightarrow \mu^+ \mu^-)$ +jets control sample is used to measure the correction factor for the modeling of the VBF selection efficiency in W +jets events. The correction factor $SF_{W+jets}^{\text{CR2}}(\text{VBF})$ determined from the $CR2_W$ control sample is measured to be 1.18 ± 0.09 (correlations between the uncertainties of SF_{W+jets}^{CR2} and SF_{Z+jets}^{CR2} are taken into account). To validate the correction factors, the W +jets rate in samples with $m_T < 110$ GeV is scaled by $SF_{W+jets}^{\text{CR1}}(\text{central})$ and $SF_{W+jets}^{\text{CR2}}(\text{VBF})$, and agreement between the data and the corrected W +jets prediction from simulation is observed.

In the $0\ell jj$ channel, $W(\rightarrow \ell \nu_\ell)$ +jets events can enter the SR, because of the contribution to \vec{p}_T^{miss} from the neutrino, if the accompanying charged lepton fails the lepton veto criteria. To determine the contribution of $W(\rightarrow \ell \nu_\ell)$ +jets background to the $0\ell jj$ SR, a similar procedure to the $Z(\rightarrow \nu \bar{\nu})$ +jets background estimation methodology is used. The muon veto is replaced with a one-muon requirement to obtain a $W(\rightarrow \mu \nu_\mu)$ plus two jets sample, requiring $60 < m_T(\mu, \vec{p}_T^{\text{miss}}) < 100$ GeV, treating the muon as undetected, and requiring $p_T^{\text{miss}} > 250$ GeV as in the SR selection. The simulated samples are used to demonstrate that substituting the muon veto for a one-muon requirement does not affect the shapes of the \vec{p}_T^{miss} and VBF jet kinematic distributions. The measured data-over-simulation correction factor is 0.90 ± 0.02 (stat). The control region is obtained by adding the VBF topology selection, and has a measured data-over-simulation correction factor of 0.90 ± 0.08 (stat).

The QCD multijet background is only important in the $0\ell jj$ and $\tau_h jj$ channels. Among the main discriminating variables against QCD multijet events are the VBF selection criteria, the minimum separation between \vec{p}_T^{miss} and any jet $|\Delta\phi_{\min}(\vec{p}_T^{\text{miss}}, j)|$, and τ_h isolation. Thus, the QCD multijet background estimation methodology utilizes CRs obtained by inverting these requirements. In the $\tau_h jj$ channel, the QCD multijet background is estimated using a completely data-driven approach which relies on the matrix (“ABCD”) method. The regions are defined as follows:

- **CRA**: inverted VBF selection; pass the nominal (tight) τ_h isolation;
- **CRB**: inverted VBF selection; fail the nominal τ_h isolation but pass loose τ_h isolation;

- *CRC*: pass the VBF selection; fail the nominal τ_h isolation but pass loose τ_h isolation and;
- *CRD*: pass the VBF selection; pass the nominal τ_h isolation

The QCD multijet component N_{QCD}^i in regions $i = \text{CRA}, \text{CRB}, \text{CRC}$ is estimated by subtracting non-QCD backgrounds (predicted using simulation) from data ($N_{\text{QCD}}^i = N_{\text{Data}}^i - N_{\neq\text{QCD}}^i$). The QCD multijet component in *CRD* (i.e., the SR) is then estimated to be $N_{\text{QCD}}^{\text{SR}} = N_{\text{QCD}}^{\text{CRA}} N_{\text{QCD}}^{\text{CRC}} / N_{\text{QCD}}^{\text{CRB}}$, where $N_{\text{QCD}}^{\text{CRC}} / N_{\text{QCD}}^{\text{CRB}}$ is referred to as the “pass-to-fail VBF” transfer factor (TF_{VBF}). Said differently, the yield of QCD multijet events in data with an inverted VBF selection is extrapolated to the SR using the transfer factor TF_{VBF} , which is measured in data samples enriched with QCD multijet events that fail the nominal τ_h isolation criteria but satisfy the loose τ_h isolation working point (henceforth referred to as “inverted τ_h isolation” or “nonisolated τ_h ”). The purity of the QCD multijet events is approximately 53–77% depending on the CR. The shape of the $m_{\text{T}}(\tau_h, p_{\text{T}}^{\text{miss}})$ distribution is obtained from *CRB* (from the nonisolated τ_h plus inverted VBF control sample). This “ABCD” method relies on TF_{VBF} being unbiased by the τ_h isolation requirement. A closure test of this assumption is provided using the simulated QCD multijet samples, resulting in agreement at a 5% level and within the statistical uncertainties.

In the $0\ell\text{jj}$ channel, the contribution from QCD multijet production is estimated using the number of events passing the analysis selection except the $|\Delta\phi_{\text{min}}(\vec{p}_{\text{T}}^{\text{miss}}, j)|$ requirement. The QCD multijet purity in this CR is about 74% according to simulation. The m_{jj} distribution of the non-QCD background is subtracted from the m_{jj} data distribution, and the resultant QCD multijet m_{jj} distribution from data is scaled by the efficiency to inefficiency ratio of the $|\Delta\phi_{\text{min}}(\vec{p}_{\text{T}}^{\text{miss}}, j)|$ requirement, $TF_{\Delta\phi}$. The transfer factor $TF_{\Delta\phi} = 0.06 \pm 0.01$ is determined using the simulated QCD multijet samples and validated using data control samples obtained by selecting events that fall in the dijet mass window $500 < m_{\text{jj}} < 1000$ GeV.

7 Systematic uncertainties

The main contributions to the total systematic uncertainty in the background predictions arise from the closure tests and from the statistical uncertainties associated with the data CRs used to determine the $SF_{\text{BG}}^{\text{CR1}}$ (central), $SF_{\text{BG}}^{\text{CR2}}$ (VBF), TF_{VBF} , and $TF_{\Delta\phi}$ factors. The relative systematic uncertainties on the product $SF_{\text{BG}}^{\text{CR1}}$ (central) $SF_{\text{BG}}^{\text{CR2}}$ (VBF) related to the statistical precision in the CRs range between 8 and 42%, depending on the background component and search channel. For TF_{VBF} and $TF_{\Delta\phi}$, the statistical uncertainties lie between 13 and 22%. The systematic uncertainties in the $SF_{\text{BG}}^{\text{CR1}}$ (central), $SF_{\text{BG}}^{\text{CR2}}$ (VBF), TF_{VBF} , and $TF_{\Delta\phi}$ factors, evaluated from the closure tests and cross-checks with data, range from 9 to 33%, depending on the channel. Additionally, although the background m_{T} and m_{jj} shapes between data and simulation are consistent within statistical uncertainties, data/BG ratios of the m_{T} and m_{jj} distributions are fit with a first-order polynomial, and the deviation of the fit from unity, as a function of m_{T} or m_{jj} , is conservatively taken as the systematic uncertainty on the shape. This results in up to $\approx 10\%$ systematic uncertainty in a given m_{T} or m_{jj} bin.

Less significant contributions to the systematic uncertainties arise from contamination by non-targeted background sources to the CRs used to measure $SF_{\text{BG}}^{\text{CR1}}$ (central) and $SF_{\text{BG}}^{\text{CR2}}$ (VBF), and from the uncertainties in these correction factors caused by uncertainties in the lepton identification efficiency, lepton energy and momentum scales, $p_{\text{T}}^{\text{miss}}$ scale, and trigger efficiency.

The efficiencies for the electron and muon reconstruction, identification, and isolation requirements are measured with the “tag-and-probe” method [33, 34] with a resulting uncertainty of $\leq 2\%$, dependent on p_{T} and η . The total efficiency for the τ_{h} identification and isolation requirements is measured from a fit to the $Z \rightarrow \tau\tau \rightarrow \mu\tau_{\text{h}}$ visible mass distribution in a sample selected with one isolated muon trigger candidate with $p_{\text{T}} > 24$ GeV, leading to a relative uncertainty of 5% per τ_{h} candidate [35]. The $p_{\text{T}}^{\text{miss}}$ scale uncertainties contribute via the jet energy scale (2–5% depending on η and p_{T}) and unclustered energy scale (10%) uncertainties, where “unclustered energy” refers to energy from a reconstructed object that is not assigned to a jet with $p_{\text{T}} > 10$ GeV or to a lepton with $p_{\text{T}} > 10$ GeV. A $p_{\text{T}}^{\text{miss}}$ -dependent uncertainty in the measured trigger efficiency results in a 3% uncertainty in the signal and background predictions that rely on simulation. The trigger efficiency is measured by calculating the fraction of W+jets events (selected with the same single- μ trigger), that also pass the same trigger that is used to define the SR.

The signal and minor backgrounds, estimated solely from simulation, are affected by similar sources of systematic uncertainty. For example, the uncertainties in the lepton identification efficiency, lepton energy and momentum scale, $p_{\text{T}}^{\text{miss}}$ scale, trigger efficiency, and integrated luminosity uncertainty of 2.5% [59] also contribute to the systematic uncertainty in the signal.

The signal event acceptance for the VBF selection depends on the reconstruction and identification efficiency and jet energy scale of forward jets. The total efficiency for the jet reconstruction and identification requirements is $> 98\%$ for the entire η and p_{T} range, as validated through the agreement observed between data and simulation in the η distribution of jets, in particular at high η , in CRs enriched with $t\bar{t}$ background events. Among the dominant uncertainties in the signal acceptance is the modeling of the kinematic properties of jets, and thus the efficiency to select VBF topologies for forward jets in the MADGRAPH simulation. This is investigated by comparing the predicted and measured m_{jj} spectra in the Z+jets CRs. The level of agreement between the predicted and observed m_{jj} spectra is better than 9%, which is assigned as a systematic uncertainty in the VBF efficiency for signal samples. The dominant uncertainty in the signal acceptance arises from the partial mistiming of signals in the forward region of the ECAL endcaps, which led to a reduction in the L1 trigger efficiency. A correction for this effect was determined using an unbiased data sample. This correction was found to be about 8% for m_{jj} of 1 TeV and increases to about 19% for m_{jj} greater than 3.5 TeV. The uncertainty in the signal acceptance from the PDF set used in simulation is evaluated in accordance with the PDF4LHC recommendations [60] by comparing the results obtained using the CTEQ6.6L, MSTW08, and NNPDF10 PDF sets [61–63] with those from the default PDF set. It should be noted that the combined uncertainty on the signal yields and $m_{\text{jj}}/m_{\text{T}}$ shapes due to scale variations on renormalization, factorization, and jet matching is found to be about 2%, which is small

Process	μ_{jj}	e_{jj}	τ_{hjj}	$0\ell jj$
DY+jets	0.20 ± 0.07	0.10 ± 0.04	0.10 ± 0.04	3714 ± 760
W+jets	13 ± 3	6 ± 1	7 ± 2	2999 ± 620
VV	1.7 ± 0.7	1.5 ± 0.6	0.9 ± 0.9	77 ± 18
$t\bar{t}$	13 ± 4	11 ± 4	5 ± 3	577 ± 128
Single top quark	2.2 ± 0.9	0.2 ± 0.1	0.6 ± 0.3	104 ± 10
QCD	$0_{-0}^{+0.2}$	$0_{-0}^{+1.2}$	23 ± 5	546 ± 69
Total BG	31 ± 5	19 ± 5	37 ± 6	8017 ± 992
Data	36	29	38	8408

Table 1. The number of observed events and corresponding pre-fit background predictions, where “pre-fit” refers to the predictions determined as described in the text, before constraints from the fitting procedure have been applied. The uncertainties include the statistical and systematic components.

compared to our estimate of 9% using the Z+jets CRs. Other dominant uncertainties that contribute to the m_{jj} and m_T shape variations include the p_T^{miss} energy scale, τ_h energy scale, and jet energy scale uncertainties.

8 Results and interpretation

Table 1 lists the number of observed events in data as well as the predicted background contributions in the SR for each channel, integrating over m_{jj} and m_T bins. Figure 3 shows the predicted SM background, expected signal, and observed data rates in bins of m_T for the $1\ell jj$ channels and bins of m_{jj} in the $0\ell jj$ channel. The bin sizes in the distributions of figure 3 are chosen to maximize the signal significance of the analysis. No significant excess of events is observed above the SM prediction in any of the search regions. Therefore the search does not reveal any evidence for new physics.

To illustrate the sensitivity of this search, the results are presented in the context of the R -parity conserving MSSM and considering cases such as those shown in figure 1 for pure electroweak VBF production of charginos and neutralinos. As mentioned previously, models with a bino-like $\tilde{\chi}_1^0$ and wino-like $\tilde{\chi}_2^0$ and $\tilde{\chi}_1^\pm$ are considered. Since in this case the $\tilde{\chi}_2^0$ and $\tilde{\chi}_1^\pm$ belong to the same gauge group multiplet, the $\tilde{\chi}_2^0$ mass is set to $m_{\tilde{\chi}_2^0} = m_{\tilde{\chi}_1^\pm}$ and results are presented as a function of this common mass and mass difference $\Delta m \equiv m(\tilde{\chi}_2^0) - m(\tilde{\chi}_1^0)$. Two scenarios have been considered: (i) the “light slepton” model where $\tilde{\ell}$ is the next-to-lightest SUSY particle; and (ii) the “WZ” model where sleptons are too heavy and thus $\tilde{\chi}_1^\pm$ and $\tilde{\chi}_2^0$ decays proceed via W^* and Z^* . The main difference between the two models is the branching ratio of $\tilde{\chi}_1^\pm$ and $\tilde{\chi}_2^0$ to leptonic final states. It should be noted that the branching fractions to leptons are adapted to off-shell W and Z bosons. In the models shown in the top row of figure 1, the mass $m_{\tilde{\ell}}$ of the intermediate slepton is parameterized in terms of a variable $x_{\tilde{\ell}}$ as

$$m_{\tilde{\ell}} = m_{\tilde{\chi}_1^0} + x_{\tilde{\ell}}(m_{\tilde{\chi}_1^\pm} - m_{\tilde{\chi}_1^0}), \tag{8.1}$$

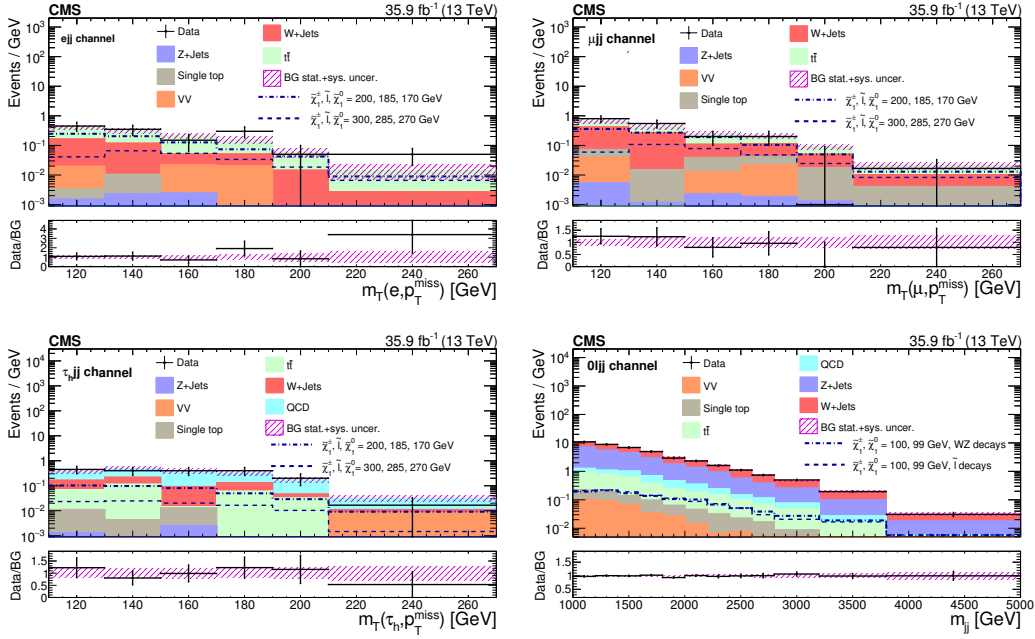


Figure 3. The observed m_T and m_{jj} distributions in the e_{jj} (upper left), μ_{jj} (upper right), τ_{hjj} (lower left), and $0l_{jj}$ (lower right) signal regions compared with the post-fit SM background yields from the fit described in the text. The pre-fit background yields and shapes are determined using data-driven methods for the major backgrounds, and based on simulation for the smaller backgrounds. Expected signal distributions are overlaid. The last bin in the m_T distributions of the $1l_{jj}$ channels include all events with $m_T > 210$ GeV. The last bin of the m_{jj} distributions of the $0l_{jj}$ channel include all events with $m_{jj} > 3800$ GeV.

where $0 < x_{\tilde{\ell}} < 1$. Results are presented for $x_{\tilde{\ell}} = 0.5$ in the “ $\tilde{\ell}$ -democratic” model where three sleptons ($m_{\tilde{\ell}} = m_{\tilde{e}} = m_{\tilde{\mu}} = m_{\tilde{\tau}}$) are light [15]. The results are interpreted by assuming branching fractions $\mathcal{B}(\tilde{\chi}_2^0 \rightarrow \ell\tilde{\ell} \rightarrow \ell\ell\tilde{\chi}_1^0) = 1$ and $\mathcal{B}(\tilde{\chi}_1^\pm \rightarrow \nu_{\ell}\tilde{\ell} \rightarrow \nu_{\ell}\ell\tilde{\chi}_1^0) = 1$. To highlight the evolution of the search sensitivity for compressed spectra with mass gap Δm , values between $\Delta m = 1$ and 50 GeV are studied for both the light slepton and WZ interpretations. The signal selection efficiency for the $1\mu_{jj}$ ($1e_{jj}$) channel in the light slepton model, assuming $\Delta m = 30$ GeV, is 0.9 (0.7)% for $m(\tilde{\chi}_1^\pm) = 100$ GeV and 2.5 (1.8)% for $m(\tilde{\chi}_1^\pm) = 300$ GeV. Similarly, the signal selection efficiency for the $0l_{jj}$ channel, assuming $\Delta m = 1$ GeV, is 2.8% for $m(\tilde{\chi}_1^\pm) = 100$ GeV and 5.3% for $m(\tilde{\chi}_1^\pm) = 300$ GeV.

The calculation of the exclusion limit is obtained by using the m_T (m_{jj}) distribution in the $1l_{jj}$ ($0l_{jj}$) to construct a combined profile likelihood ratio test statistic [64] in bins of m_T (m_{jj}) and computing a 95% confidence level (CL) upper limit (UL) on the signal cross section using the asymptotic CL_s criterion [64–66]. Systematic uncertainties are taken into account as nuisance parameters, which are removed by profiling, assuming gamma function or log-normal priors for normalization parameters, and Gaussian priors for mass spectrum shape uncertainties. The combination of the four search channels requires simultaneous analysis of the data from the individual channels, accounting for all statistical and systematic uncertainties and their correlations. Correlations among backgrounds, both

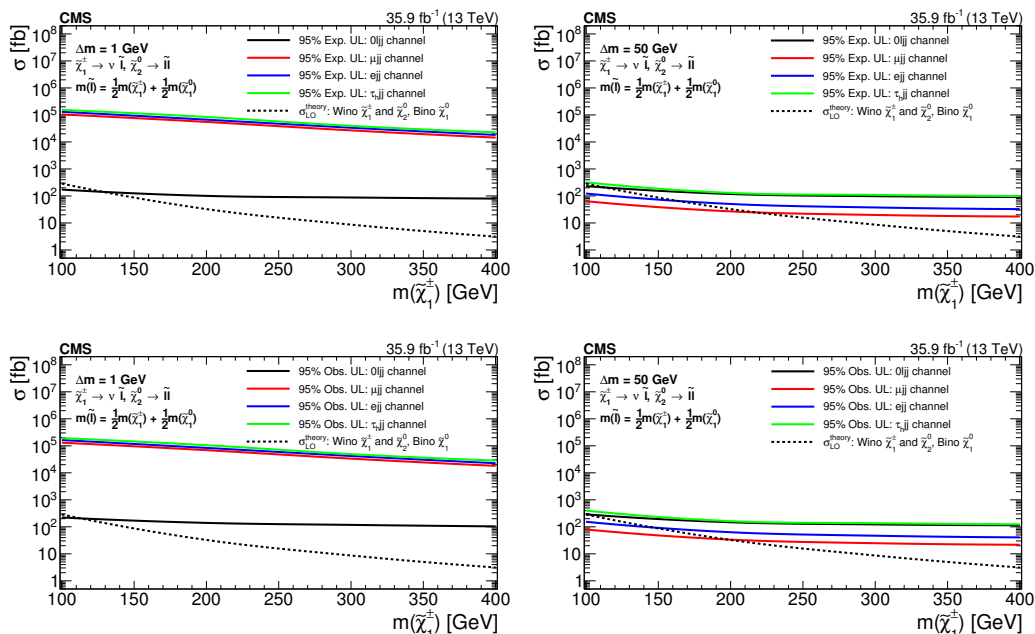


Figure 4. Combined 95% CL UL on the cross section as a function of $m_{\tilde{\chi}_2^\pm} = m_{\tilde{\chi}_1^\pm}$. The results correspond to $\Delta m = 1$ GeV (left) and $\Delta m = 50$ GeV (right) mass gaps between the chargino and the lightest neutralino in the light slepton model. The top row shows the expected limits, and the bottom row shows the observed limits.

within a channel and across channels, are taken into consideration in the limit calculation. For example, the uncertainty in the integrated luminosity is treated as fully correlated across channels. The uncertainties in the predicted signal yields resulting from the event acceptance variation with different sets of PDFs in a given m_T or m_{jj} bin are treated as uncorrelated within a channel and correlated across channels. The uncertainties from the closure tests are treated as uncorrelated within and across the different final states.

Figure 4 shows the expected and observed limits as well as the theoretical cross section as functions of $m_{\tilde{\chi}_1^\pm}$ for the $\Delta m = 1$ and 50 GeV assumptions in the light slepton model. For the smallest value of $\Delta m = 1$ GeV, the $0ljj$ channel provides the best sensitivity, while the VBF soft- e and soft- μ channels provide the best sensitivity for the larger mass gap scenario with $\Delta m = 50$ GeV. The four channels are combined and the results are presented in figure 5. Figure 5 (left) shows the 95% CL UL on the signal cross section, as a function of $m(\tilde{\chi}_1^\pm)$ and Δm , assuming $x_{\tilde{\chi}} = 0.5$. Figure 5 (right) shows the 95% CL UL on the signal cross section, as a function of $m(\tilde{\chi}_1^\pm)$, for two fixed Δm values of 1 and 30 GeV, and assuming $x_{\tilde{\chi}} = 0.5$. The signal acceptance and mass shape are evaluated for each $\{m(\tilde{\chi}_1^\pm), \Delta m\}$ combination and used in the limit calculation procedure described above. For the $\Delta m = \{1, 10, 30, 50\}$ GeV assumption, the combination of the four channels results in an observed (expected) exclusion on the $\tilde{\chi}_2^0$ and $\tilde{\chi}_1^\pm$ gaugino masses below $\{112, 159, 215, 207\}$ ($\{125, 171, 235, 228\}$) GeV. For the compressed mass spectrum scenarios with $1 \leq \Delta m \leq 30$ GeV, the bounds on the $\tilde{\chi}_2^0$ and $\tilde{\chi}_1^\pm$ gaugino masses are the most stringent to date.

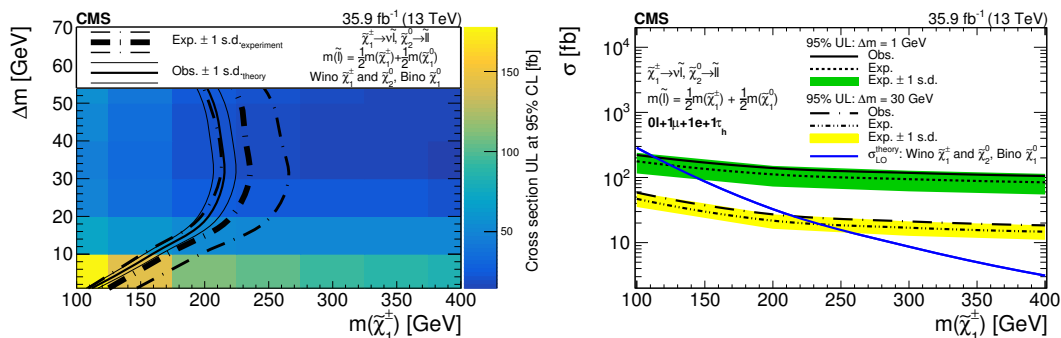


Figure 5. (Left) Expected and observed 95% confidence level upper limit (UL) on the signal cross section as a function of $m(\tilde{\chi}_1^\pm)$ and Δm , assuming the light slepton model with slepton mass defined as the average of the $\tilde{\chi}_2^0$ and $\tilde{\chi}_1^\pm$ masses, $x_{\tilde{\ell}} = 0.5$. The lower left edge of each bin represents the $\{m(\tilde{\chi}_1^\pm), \Delta m\}$ combination used to calculate the UL on the signal cross section. For example, the lowest and leftmost bin corresponds to the UL on the signal cross section for the scenario with $m(\tilde{\chi}_1^\pm) = 100$ GeV and $\Delta m = 1$ GeV. (Right) Combined 95% CL UL on the cross section as a function of $m_{\tilde{\chi}_2^0} = m_{\tilde{\chi}_1^\pm}$, for $\Delta m = 1$ GeV and $\Delta m = 30$ GeV mass gaps between the chargino and the neutralino, assuming the light slepton model.

It is noted that for the $1 < \Delta m < 10$ GeV mass gaps considered in this analysis, the exclusions on $m(\tilde{\chi}_1^\pm)$ do not depend on the assumption that a light slepton exists (i.e. $m(\tilde{\chi}_1^0) < m_{\tilde{\ell}} < m(\tilde{\chi}_1^\pm)$). For $1 < \Delta m < 10$ GeV, the signal acceptance for the WZ model is similar to the signal acceptance for the light slepton model. For example, figure 3 (lower right) shows the expected m_{jj} signal distribution when the decays of the charginos and neutralinos proceed via W and Z bosons, resulting in a similar shape and normalization as the expectation for the light slepton scenario. However, for increasing Δm values where the $1\ell jj$ channels dominate the sensitivity, the exclusions on $m(\tilde{\chi}_1^\pm)$ in the WZ model are less stringent than the ones in the light slepton model. This difference is a result of the lower branching ratio of $\tilde{\chi}_1^\pm$ and $\tilde{\chi}_2^0$ to leptonic final states in the WZ model.

Figure 6 (left) shows the 95% CL UL on the signal cross section, as a function of $m(\tilde{\chi}_1^\pm)$ and Δm , assuming the WZ model. Figure 6 (right) shows the 95% CL UL on the signal cross section, as a function of $m(\tilde{\chi}_1^\pm)$, for two fixed Δm values of 1 and 30 GeV, and assuming the WZ model. For the $\Delta m = \{1, 10, 30, 50\}$ GeV assumption, the combination of the four channels results in an observed (expected) exclusion on the $\tilde{\chi}_2^0$ and $\tilde{\chi}_1^\pm$ gaugino masses below $\{112, 146, 175, 162\}$ ($\{125, 160, 194, 178\}$) GeV. For the compressed mass spectrum scenarios with $1 \leq \Delta m < 3$ GeV and $25 \leq \Delta m < 50$ GeV, the bounds on the $\tilde{\chi}_2^0$ and $\tilde{\chi}_1^\pm$ gaugino masses in the WZ model are also the most stringent to date, surpassing the bounds from the LEP experiments [67–70].

9 Summary

A search is presented for noncolored supersymmetric particles produced in the vector boson fusion (VBF) topology using data corresponding to an integrated luminosity of 35.9 fb^{-1} collected in 2016 with the CMS detector in proton-proton collisions at $\sqrt{s} = 13$ TeV. The search utilizes events in four different channels depending on the number and type of

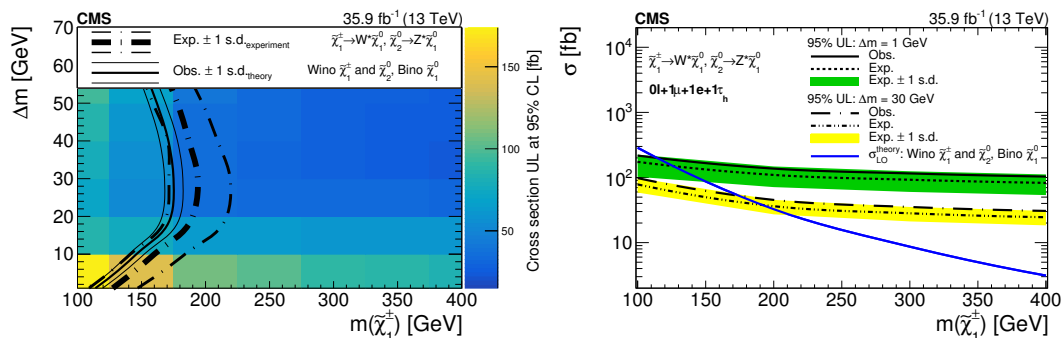


Figure 6. (Left) Expected and observed 95% confidence level upper limit (UL) on the signal cross section as a function of $m(\tilde{\chi}_1^\pm)$ and Δm , assuming the $\tilde{\chi}_1^\pm$ and $\tilde{\chi}_2^0$ decays proceed via W^* and Z^* . The lower left edge of each bin represents the $\{m(\tilde{\chi}_1^\pm), \Delta m\}$ combination used to calculate the UL on the signal cross section. For example, the lowest and leftmost bin corresponds to the UL on the signal cross section for the scenario with $m(\tilde{\chi}_1^\pm) = 100$ GeV and $\Delta m = 1$ GeV. (Right) The 95% CL UL on the cross section as a function of $m_{\tilde{\chi}_2^0} = m_{\tilde{\chi}_1^\pm}$, for $\Delta m = 1$ GeV and $\Delta m = 30$ GeV mass gaps between the chargino and the neutralino, after combining 0 lepton and 1 lepton channels, assuming the $\tilde{\chi}_1^\pm$ and $\tilde{\chi}_2^0$ decays proceed via W^* and Z^* .

leptons: $0\ell jj$, $e jj$, μjj , and τ_{hjj} , where τ_h denotes a hadronically decaying τ lepton. While ref. [71] reported a search using the VBF dijet topology with a zero-lepton final state in proton-proton collision data at $\sqrt{s} = 8$ TeV, this is the first search for the compressed electroweak supersymmetry (SUSY) sector using the $0\ell jj$ final state. This is also the first search for SUSY in the VBF topology with single soft-lepton final states. The VBF topology requires two well-separated jets that appear in opposite hemispheres, with large invariant mass m_{jj} . The observed m_{jj} and transverse mass $m_T(\ell, p_T^{\text{miss}})$ distributions do not reveal any evidence for new physics. The results are used to exclude a range of $\tilde{\chi}_1^\pm$ and $\tilde{\chi}_2^0$ gaugino masses. For a compressed mass spectrum scenario, in which $\Delta m \equiv m(\tilde{\chi}_1^\pm) - m(\tilde{\chi}_1^0) = 1$ (30) GeV and in which $\tilde{\chi}_1^\pm$ and $\tilde{\chi}_2^0$ branching fractions to light sleptons are 100%, $\tilde{\chi}_1^\pm$ and $\tilde{\chi}_2^0$ masses up to 112 (215) GeV are excluded at 95% CL. For the scenario where the sleptons are too heavy and decays of the charginos and neutralinos proceed via W^* and Z^* bosons, $\tilde{\chi}_1^\pm$ and $\tilde{\chi}_2^0$ masses up to 112 (175) GeV are excluded at 95% CL for $\Delta m = 1$ (30) GeV. While many previous studies at the LHC have focused on strongly coupled supersymmetric particles, including searches for charginos and neutralinos produced in gluino or squark decay chains, and a number of studies have presented limits on the Drell-Yan production of charginos and neutralinos, this analysis obtains the most stringent limits to date on the production of charginos and neutralinos decaying to leptons in compressed mass spectrum scenarios defined by the mass separation $1 \leq \Delta m < 3$ GeV and $25 \leq \Delta m < 50$ GeV.

Acknowledgments

We congratulate our colleagues in the CERN accelerator departments for the excellent performance of the LHC and thank the technical and administrative staffs at CERN and at other CMS institutes for their contributions to the success of the CMS effort. In addition, we gratefully acknowledge the computing centers and personnel of the Worldwide LHC

Computing Grid for delivering so effectively the computing infrastructure essential to our analyses. Finally, we acknowledge the enduring support for the construction and operation of the LHC and the CMS detector provided by the following funding agencies: BMBWF and FWF (Austria); FNRS and FWO (Belgium); CNPq, CAPES, FAPERJ, FAPERGS, and FAPESP (Brazil); MES (Bulgaria); CERN; CAS, MoST, and NSFC (China); COLCIENCIAS (Colombia); MSES and CSF (Croatia); RPF (Cyprus); SENESCYT (Ecuador); MoER, ERC IUT, PUT and ERDF (Estonia); Academy of Finland, MEC, and HIP (Finland); CEA and CNRS/IN2P3 (France); BMBF, DFG, and HGF (Germany); GSRT (Greece); NKFI (Hungary); DAE and DST (India); IPM (Iran); SFI (Ireland); INFN (Italy); MSIP and NRF (Republic of Korea); MES (Latvia); LAS (Lithuania); MOE and UM (Malaysia); BUAP, CINVESTAV, CONACYT, LNS, SEP, and UASLP-FAI (Mexico); MOS (Montenegro); MBIE (New Zealand); PAEC (Pakistan); MSHE and NSC (Poland); FCT (Portugal); JINR (Dubna); MON, RosAtom, RAS, RFBR, and NRC KI (Russia); MESTD (Serbia); SEIDI, CPAN, PCTI, and FEDER (Spain); MOSTR (Sri Lanka); Swiss Funding Agencies (Switzerland); MST (Taipei); ThEPCenter, IPST, STAR, and NSTDA (Thailand); TUBITAK and TAEK (Turkey); NASU and SFFR (Ukraine); STFC (United Kingdom); DOE and NSF (U.S.A.).

Individuals have received support from the Marie-Curie program and the European Research Council and Horizon 2020 Grant, contract Nos. 675440, 752730, and 765710 (European Union); the Leventis Foundation; the A.P. Sloan Foundation; the Alexander von Humboldt Foundation; the Belgian Federal Science Policy Office; the Fonds pour la Formation à la Recherche dans l’Industrie et dans l’Agriculture (FRIA-Belgium); the Agentschap voor Innovatie door Wetenschap en Technologie (IWT-Belgium); the F.R.S.-FNRS and FWO (Belgium) under the “Excellence of Science — EOS” — be.h project n. 30820817; the Beijing Municipal Science & Technology Commission, No. Z181100004218003; the Ministry of Education, Youth and Sports (MEYS) of the Czech Republic; the Lendület (“Momentum”) Program and the János Bolyai Research Scholarship of the Hungarian Academy of Sciences, the New National Excellence Program ÚNKP, the NKFI research grants 123842, 123959, 124845, 124850, 125105, 128713, 128786, and 129058 (Hungary); the Council of Science and Industrial Research, India; the HOMING PLUS program of the Foundation for Polish Science, cofinanced from European Union, Regional Development Fund, the Mobility Plus program of the Ministry of Science and Higher Education, the National Science Center (Poland), contracts Harmonia 2014/14/M/ST2/00428, Opus 2014/13/B/ST2/02543, 2014/15/B/ST2/03998, and 2015/19/B/ST2/02861, Sonata-bis 2012/07/E/ST2/01406; the National Priorities Research Program by Qatar National Research Fund; the Ministry of Science and Education, grant no. 3.2989.2017 (Russia); the Programa Estatal de Fomento de la Investigación Científica y Técnica de Excelencia María de Maeztu, grant MDM-2015-0509 and the Programa Severo Ochoa del Principado de Asturias; the Thalís and Aristeia programs cofinanced by EU-ESF and the Greek NSRF; the Rachadapisek Sompot Fund for Postdoctoral Fellowship, Chulalongkorn University and the Chulalongkorn Academic into Its 2nd Century Project Advancement Project (Thailand); the Welch Foundation, contract C-1845; and the Weston Havens Foundation (U.S.A.).

Open Access. This article is distributed under the terms of the Creative Commons Attribution License ([CC-BY 4.0](https://creativecommons.org/licenses/by/4.0/)), which permits any use, distribution and reproduction in any medium, provided the original author(s) and source are credited.

References

- [1] P. Ramond, *Dual theory for free fermions*, *Phys. Rev. D* **3** (1971) 2415 [[INSPIRE](#)].
- [2] Yu. A. Golfand and E.P. Likhtman, *Extension of the algebra of Poincaré group generators and violation of p invariance*, *JETP Lett.* **13** (1971) 323 [[INSPIRE](#)].
- [3] S. Ferrara and B. Zumino, *Supergauge invariant Yang-Mills theories*, *Nucl. Phys. B* **79** (1974) 413 [[INSPIRE](#)].
- [4] J. Wess and B. Zumino, *Supergauge transformations in four-dimensions*, *Nucl. Phys. B* **70** (1974) 39 [[INSPIRE](#)].
- [5] A.H. Chamseddine, R.L. Arnowitt and P. Nath, *Locally supersymmetric grand unification*, *Phys. Rev. Lett.* **49** (1982) 970 [[INSPIRE](#)].
- [6] R. Barbieri, S. Ferrara and C.A. Savoy, *Gauge models with spontaneously broken local supersymmetry*, *Phys. Lett.* **119B** (1982) 343 [[INSPIRE](#)].
- [7] L.J. Hall, J.D. Lykken and S. Weinberg, *Supergravity as the messenger of supersymmetry breaking*, *Phys. Rev. D* **27** (1983) 2359 [[INSPIRE](#)].
- [8] CMS collaboration, *Search for new phenomena with the M_{T2} variable in the all-hadronic final state produced in proton-proton collisions at $\sqrt{s} = 13$ TeV*, *Eur. Phys. J. C* **77** (2017) 710 [[arXiv:1705.04650](#)] [[INSPIRE](#)].
- [9] CMS collaboration, *Search for supersymmetry in multijet events with missing transverse momentum in proton-proton collisions at 13 TeV*, *Phys. Rev. D* **96** (2017) 032003 [[arXiv:1704.07781](#)] [[INSPIRE](#)].
- [10] ATLAS collaboration, *Search for squarks and gluinos in events with an isolated lepton, jets and missing transverse momentum at $\sqrt{s} = 13$ TeV with the ATLAS detector*, *Phys. Rev. D* **96** (2017) 112010 [[arXiv:1708.08232](#)] [[INSPIRE](#)].
- [11] ATLAS collaboration, *Search for squarks and gluinos in final states with jets and missing transverse momentum using 36 fb^{-1} of $\sqrt{s} = 13$ TeV pp collision data with the ATLAS detector*, *Phys. Rev. D* **97** (2018) 112001 [[arXiv:1712.02332](#)] [[INSPIRE](#)].
- [12] J. Alwall, P. Schuster and N. Toro, *Simplified models for a first characterization of new physics at the LHC*, *Phys. Rev. D* **79** (2009) 075020 [[arXiv:0810.3921](#)] [[INSPIRE](#)].
- [13] LHC NEW PHYSICS WORKING GROUP collaboration, *Simplified models for LHC new physics searches*, *J. Phys. G* **39** (2012) 105005 [[arXiv:1105.2838](#)] [[INSPIRE](#)].
- [14] G.R. Farrar and P. Fayet, *Phenomenology of the production, decay and detection of new hadronic states associated with supersymmetry*, *Phys. Lett.* **76B** (1978) 575 [[INSPIRE](#)].
- [15] CMS collaboration, *Combined search for electroweak production of charginos and neutralinos in proton-proton collisions at $\sqrt{s} = 13$ TeV*, *JHEP* **03** (2018) 160 [[arXiv:1801.03957](#)] [[INSPIRE](#)].
- [16] ATLAS collaboration, *Search for electroweak production of supersymmetric particles in final states with two or three leptons at $\sqrt{s} = 13$ TeV with the ATLAS detector*, *Eur. Phys. J. C* **78** (2018) 995 [[arXiv:1803.02762](#)] [[INSPIRE](#)].

- [17] ATLAS collaboration, *Search for chargino-neutralino production using recursive jigsaw reconstruction in final states with two or three charged leptons in proton-proton collisions at $\sqrt{s} = 13$ TeV with the ATLAS detector*, *Phys. Rev. D* **98** (2018) 092012 [[arXiv:1806.02293](#)] [[INSPIRE](#)].
- [18] ATLAS collaboration, *Search for electroweak production of supersymmetric states in scenarios with compressed mass spectra at $\sqrt{s} = 13$ TeV with the ATLAS detector*, *Phys. Rev. D* **97** (2018) 052010 [[arXiv:1712.08119](#)] [[INSPIRE](#)].
- [19] CMS collaboration, *Search for new physics in events with two soft oppositely charged leptons and missing transverse momentum in proton-proton collisions at $\sqrt{s} = 13$ TeV*, *Phys. Lett. B* **782** (2018) 440 [[arXiv:1801.01846](#)] [[INSPIRE](#)].
- [20] B. Dutta et al., *Vector boson fusion processes as a probe of supersymmetric electroweak sectors at the LHC*, *Phys. Rev. D* **87** (2013) 035029 [[arXiv:1210.0964](#)] [[INSPIRE](#)].
- [21] G.F. Giudice, T. Han, K. Wang and L.-T. Wang, *Nearly degenerate gauginos and dark matter at the LHC*, *Phys. Rev. D* **81** (2010) 115011 [[arXiv:1004.4902](#)] [[INSPIRE](#)].
- [22] A.G. Delannoy et al., *Probing dark matter at the LHC using vector boson fusion processes*, *Phys. Rev. Lett.* **111** (2013) 061801 [[arXiv:1304.7779](#)] [[INSPIRE](#)].
- [23] CMS collaboration, *Search for supersymmetry in the vector-boson fusion topology in proton-proton collisions at $\sqrt{s} = 8$ TeV*, *JHEP* **11** (2015) 189 [[arXiv:1508.07628](#)] [[INSPIRE](#)].
- [24] CMS collaboration, *The CMS experiment at the CERN LHC, 2008* *JINST* **3** S08004 [[INSPIRE](#)].
- [25] CMS collaboration, *Particle-flow reconstruction and global event description with the CMS detector, 2017* *JINST* **12** P10003 [[arXiv:1706.04965](#)] [[INSPIRE](#)].
- [26] CMS collaboration, *Performance of missing energy reconstruction in 13 TeV pp collision data using the CMS detector*, *CMS-PAS-JME-16-004* (2016).
- [27] M. Cacciari, G.P. Salam and G. Soyez, *The anti- k_t jet clustering algorithm*, *JHEP* **04** (2008) 063 [[arXiv:0802.1189](#)] [[INSPIRE](#)].
- [28] M. Cacciari, G.P. Salam and G. Soyez, *FastJet user manual*, *Eur. Phys. J. C* **72** (2012) 1896 [[arXiv:1111.6097](#)] [[INSPIRE](#)].
- [29] M. Cacciari and G.P. Salam, *Pileup subtraction using jet areas*, *Phys. Lett. B* **659** (2008) 119 [[arXiv:0707.1378](#)] [[INSPIRE](#)].
- [30] CMS collaboration, *Jet energy scale and resolution in the CMS experiment in pp collisions at 8 TeV, 2017* *JINST* **12** P02014 [[arXiv:1607.03663](#)] [[INSPIRE](#)].
- [31] CMS collaboration, *Pileup jet identification*, *CMS-PAS-JME-13-005* (2013).
- [32] CMS collaboration, *Identification of heavy-flavour jets with the CMS detector in pp collisions at 13 TeV, 2018* *JINST* **13** P05011 [[arXiv:1712.07158](#)] [[INSPIRE](#)].
- [33] CMS collaboration, *Performance of the CMS muon detector and muon reconstruction with proton-proton collisions at $\sqrt{s} = 13$ TeV, 2018* *JINST* **13** P06015 [[arXiv:1804.04528](#)] [[INSPIRE](#)].
- [34] CMS collaboration, *Performance of electron reconstruction and selection with the CMS detector in proton-proton collisions at $\sqrt{s} = 8$ TeV, 2015* *JINST* **10** P06005 [[arXiv:1502.02701](#)] [[INSPIRE](#)].
- [35] CMS collaboration, *Reconstruction and identification of τ lepton decays to hadrons and ν_τ at CMS, 2016* *JINST* **11** P01019 [[arXiv:1510.07488](#)].

- [36] J. Alwall et al., *The automated computation of tree-level and next-to-leading order differential cross sections and their matching to parton shower simulations*, *JHEP* **07** (2014) 079 [[arXiv:1405.0301](#)] [[INSPIRE](#)].
- [37] CMS collaboration, *Electroweak production of two jets in association with a Z boson in proton–proton collisions at $\sqrt{s} = 13$ TeV*, *Eur. Phys. J. C* **78** (2018) 589 [[arXiv:1712.09814](#)] [[INSPIRE](#)].
- [38] R. Frederix, E. Re and P. Torrielli, *Single-top t -channel hadroproduction in the four-flavour scheme with POWHEG and aMC@NLO*, *JHEP* **09** (2012) 130 [[arXiv:1207.5391](#)] [[INSPIRE](#)].
- [39] P. Nason, *A new method for combining NLO QCD with shower Monte Carlo algorithms*, *JHEP* **11** (2004) 040 [[hep-ph/0409146](#)] [[INSPIRE](#)].
- [40] S. Frixione, P. Nason and C. Oleari, *Matching NLO QCD computations with Parton Shower simulations: the POWHEG method*, *JHEP* **11** (2007) 070 [[arXiv:0709.2092](#)] [[INSPIRE](#)].
- [41] S. Alioli, P. Nason, C. Oleari and E. Re, *A general framework for implementing NLO calculations in shower Monte Carlo programs: the POWHEG BOX*, *JHEP* **06** (2010) 043 [[arXiv:1002.2581](#)] [[INSPIRE](#)].
- [42] E. Re, *Single-top Wt -channel production matched with parton showers using the POWHEG method*, *Eur. Phys. J. C* **71** (2011) 1547 [[arXiv:1009.2450](#)] [[INSPIRE](#)].
- [43] T. Sjöstrand et al., *An introduction to PYTHIA 8.2*, *Comput. Phys. Commun.* **191** (2015) 159 [[arXiv:1410.3012](#)] [[INSPIRE](#)].
- [44] CMS collaboration, *Event generator tunes obtained from underlying event and multiparton scattering measurements*, *Eur. Phys. J. C* **76** (2016) 155 [[arXiv:1512.00815](#)] [[INSPIRE](#)].
- [45] NNPDF collaboration, *Parton distributions for the LHC Run II*, *JHEP* **04** (2015) 040 [[arXiv:1410.8849](#)] [[INSPIRE](#)].
- [46] J. Alwall et al., *Comparative study of various algorithms for the merging of parton showers and matrix elements in hadronic collisions*, *Eur. Phys. J. C* **53** (2008) 473 [[arXiv:0706.2569](#)] [[INSPIRE](#)].
- [47] S. Alioli, P. Nason, C. Oleari and E. Re, *NLO single-top production matched with shower in POWHEG: s - and t -channel contributions*, *JHEP* **09** (2009) 111 [Erratum *ibid.* **1002** (2010) 011] [[arXiv:0907.4076](#)] [[INSPIRE](#)].
- [48] M. Czakon and A. Mitov, *Top++: a program for the calculation of the top-pair cross-section at hadron colliders*, *Comput. Phys. Commun.* **185** (2014) 2930 [[arXiv:1112.5675](#)] [[INSPIRE](#)].
- [49] GEANT4 collaboration, *GEANT4 — a simulation toolkit*, *Nucl. Instrum. Meth. A* **506** (2003) 250 [[INSPIRE](#)].
- [50] CMS collaboration, *The fast simulation of the CMS detector at LHC*, *J. Phys. Conf. Ser.* **331** (2011) 032049 [[INSPIRE](#)].
- [51] B. Dutta et al., *Probing compressed bottom squarks with boosted jets and shape analysis*, *Phys. Rev. D* **92** (2015) 095009 [[arXiv:1507.01001](#)] [[INSPIRE](#)].
- [52] B. Dutta et al., *Probing compressed top squark scenarios at the LHC at 14 TeV*, *Phys. Rev. D* **90** (2014) 095022 [[arXiv:1312.1348](#)] [[INSPIRE](#)].
- [53] B. Dutta et al., *Probing compressed sleptons at the LHC using vector boson fusion processes*, *Phys. Rev. D* **91** (2015) 055025 [[arXiv:1411.6043](#)] [[INSPIRE](#)].
- [54] A. Flórez et al., *Searching for new heavy neutral gauge bosons using vector boson fusion processes at the LHC*, *Phys. Lett. B* **767** (2017) 126 [[arXiv:1609.09765](#)] [[INSPIRE](#)].

- [55] A. Flórez et al., *Expanding the reach of heavy neutrino searches at the LHC*, *Phys. Lett. B* **778** (2018) 94 [[arXiv:1708.03007](#)] [[INSPIRE](#)].
- [56] A. Flórez et al., *Probing heavy spin-2 bosons with $\gamma\gamma$ final states from vector boson fusion processes at the LHC*, *Phys. Rev. D* **99** (2019) 035034 [[arXiv:1812.06824](#)] [[INSPIRE](#)].
- [57] ATLAS collaboration, *Search for invisible Higgs boson decays in vector boson fusion at $\sqrt{s} = 13$ TeV with the ATLAS detector*, *Phys. Lett. B* **793** (2019) 499 [[arXiv:1809.06682](#)] [[INSPIRE](#)].
- [58] CMS collaboration, *Search for invisible decays of a Higgs boson produced through vector boson fusion in proton-proton collisions at $\sqrt{s} = 13$ TeV*, *Phys. Lett. B* **793** (2019) 520 [[arXiv:1809.05937](#)] [[INSPIRE](#)].
- [59] CMS collaboration, *CMS Luminosity Measurements for the 2016 Data Taking Period*, CMS-PAS-LUM-17-001 (2017).
- [60] J. Butterworth et al., *PDF4LHC recommendations for LHC Run II*, *J. Phys. G* **43** (2016) 023001 [[arXiv:1510.03865](#)] [[INSPIRE](#)].
- [61] P.M. Nadolsky et al., *Implications of CTEQ global analysis for collider observables*, *Phys. Rev. D* **78** (2008) 013004 [[arXiv:0802.0007](#)] [[INSPIRE](#)].
- [62] A.D. Martin, W.J. Stirling, R.S. Thorne and G. Watt, *Update of parton distributions at NNLO*, *Phys. Lett. B* **652** (2007) 292 [[arXiv:0706.0459](#)] [[INSPIRE](#)].
- [63] M. Ubiali, *NNPDF1.0 parton set for the LHC*, *Nucl. Phys. Proc. Suppl.* **186** (2009) 62 [[arXiv:0809.3716](#)] [[INSPIRE](#)].
- [64] G. Cowan, K. Cranmer, E. Gross and O. Vitells, *Asymptotic formulae for likelihood-based tests of new physics*, *Eur. Phys. J. C* **71** (2011) 1554 [*Erratum ibid.* **C 73** (2013) 2501] [[arXiv:1007.1727](#)] [[INSPIRE](#)].
- [65] T. Junk, *Confidence level computation for combining searches with small statistics*, *Nucl. Instrum. Meth. A* **434** (1999) 435 [[hep-ex/9902006](#)] [[INSPIRE](#)].
- [66] A.L. Read, *Presentation of search results: The $CL(s)$ technique*, *J. Phys. G* **28** (2002) 2693 [[INSPIRE](#)].
- [67] ALEPH collaboration, *Absolute mass lower limit for the lightest neutralino of the MSSM from e^+e^- data at \sqrt{s} up to 209 GeV*, *Phys. Lett. B* **583** (2004) 247 [[INSPIRE](#)].
- [68] ALEPH collaboration, *Search for charginos nearly mass degenerate with the lightest neutralino in e^+e^- collisions at center-of-mass energies up to 209 GeV*, *Phys. Lett. B* **533** (2002) 223 [[hep-ex/0203020](#)] [[INSPIRE](#)].
- [69] OPAL collaboration, *Search for nearly mass degenerate charginos and neutralinos at LEP*, *Eur. Phys. J. C* **29** (2003) 479 [[hep-ex/0210043](#)] [[INSPIRE](#)].
- [70] L3 collaboration, *Search for charginos with a small mass difference with the lightest supersymmetric particle at $\sqrt{s} = 189$ GeV*, *Phys. Lett. B* **482** (2000) 31 [[hep-ex/0002043](#)] [[INSPIRE](#)].
- [71] CMS collaboration, *Search for dark matter and supersymmetry with a compressed mass spectrum in the vector boson fusion topology in proton-proton collisions at $\sqrt{s} = 8$ TeV*, *Phys. Rev. Lett.* **118** (2017) 021802 [[arXiv:1605.09305](#)] [[INSPIRE](#)].

The CMS collaboration

Yerevan Physics Institute, Yerevan, Armenia

A.M. Sirunyan, A. Tumasyan

Institut für Hochenergiephysik, Wien, Austria

W. Adam, F. Ambrogio, E. Asilar, T. Bergauer, J. Brandstetter, M. Dragicevic, J. Erö, A. Escalante Del Valle, M. Flechl, R. Frühwirth¹, V.M. Ghete, J. Hrubec, M. Jeitler¹, N. Krammer, I. Krätschmer, D. Liko, T. Madlener, I. Mikulec, N. Rad, H. Rohringer, J. Schieck¹, R. Schöfbeck, M. Spanring, D. Spitzbart, W. Waltenberger, J. Wittmann, C.-E. Wulz¹, M. Zarucki

Institute for Nuclear Problems, Minsk, Belarus

V. Chekhovsky, V. Mossolov, J. Suarez Gonzalez

Universiteit Antwerpen, Antwerpen, Belgium

E.A. De Wolf, D. Di Croce, X. Janssen, J. Lauwers, A. Lelek, M. Pieters, H. Van Haevermaet, P. Van Mechelen, N. Van Remortel

Vrije Universiteit Brussel, Brussel, Belgium

F. Blekman, J. D'Hondt, J. De Clercq, K. Deroover, G. Flouris, D. Lontkovskyi, S. Lowette, I. Marchesini, S. Moortgat, L. Moreels, Q. Python, K. Skovpen, S. Tavernier, W. Van Doninck, P. Van Mulders, I. Van Parijs

Université Libre de Bruxelles, Bruxelles, Belgium

D. Beghin, B. Bilin, H. Brun, B. Clerbaux, G. De Lentdecker, H. Delannoy, B. Dorney, G. Fasanella, L. Favart, A. Grebenyuk, A.K. Kalsi, J. Luetic, N. Postiau, E. Starling, L. Thomas, C. Vander Velde, P. Vanlaer, D. Vannerom, Q. Wang

Ghent University, Ghent, Belgium

T. Cornelis, D. Dobur, A. Fagot, M. Gul, I. Khvastunov², C. Roskas, D. Trocino, M. Tytgat, W. Verbeke, B. Vermassen, M. Vit, N. Zaganidis

Université Catholique de Louvain, Louvain-la-Neuve, Belgium

H. Bakhshiansohi, O. Bondu, G. Bruno, C. Caputo, P. David, C. Delaere, M. Delcourt, A. Giammanco, G. Krintiras, V. Lemaitre, A. Magitteri, K. Piotrkowski, A. Saggio, M. Vidal Marono, P. Vischia, J. Zobec

Centro Brasileiro de Pesquisas Fisicas, Rio de Janeiro, Brazil

F.L. Alves, G.A. Alves, G. Correia Silva, C. Hensel, A. Moraes, M.E. Pol, P. Rebello Teles

Universidade do Estado do Rio de Janeiro, Rio de Janeiro, Brazil

E. Belchior Batista Das Chagas, W. Carvalho, J. Chinellato³, E. Coelho, E.M. Da Costa, G.G. Da Silveira⁴, D. De Jesus Damiao, C. De Oliveira Martins, S. Fonseca De Souza, L.M. Huertas Guativa, H. Malbouisson, D. Matos Figueiredo, M. Melo De Almeida, C. Mora Herrera, L. Mundim, H. Nogima, W.L. Prado Da Silva, L.J. Sanchez Rosas, A. Santoro, A. Sznajder, M. Thiel, E.J. Tonelli Manganote³, F. Torres Da Silva De Araujo, A. Vilela Pereira

Universidade Estadual Paulista^a, Universidade Federal do ABC^b, São Paulo, Brazil

S. Ahuja^a, C.A. Bernardes^a, L. Calligaris^a, T.R. Fernandez Perez Tomei^a, E.M. Gregores^b, P.G. Mercadante^b, S.F. Novaes^a, SandraS. Padula^a

Institute for Nuclear Research and Nuclear Energy, Bulgarian Academy of Sciences, Sofia, Bulgaria

A. Aleksandrov, R. Hadjiiska, P. Iaydjiev, A. Marinov, M. Misheva, M. Rodozov, M. Shopova, G. Sultanov

University of Sofia, Sofia, Bulgaria

A. Dimitrov, L. Litov, B. Pavlov, P. Petkov

Beihang University, Beijing, China

W. Fang⁵, X. Gao⁵, L. Yuan

Institute of High Energy Physics, Beijing, China

M. Ahmad, J.G. Bian, G.M. Chen, H.S. Chen, M. Chen, Y. Chen, C.H. Jiang, D. Leggat, H. Liao, Z. Liu, S.M. Shaheen⁶, A. Spiezia, J. Tao, E. Yazgan, H. Zhang, S. Zhang⁶, J. Zhao

State Key Laboratory of Nuclear Physics and Technology, Peking University, Beijing, China

Y. Ban, G. Chen, A. Levin, J. Li, L. Li, Q. Li, Y. Mao, S.J. Qian, D. Wang

Tsinghua University, Beijing, China

Y. Wang

Universidad de Los Andes, Bogota, Colombia

C. Avila, A. Cabrera, C.A. Carrillo Montoya, L.F. Chaparro Sierra, C. Florez, C.F. González Hernández, M.A. Segura Delgado

Universidad de Antioquia, Medellin, Colombia

J.D. Ruiz Alvarez

University of Split, Faculty of Electrical Engineering, Mechanical Engineering and Naval Architecture, Split, Croatia

N. Godinovic, D. Lelas, I. Puljak, T. Sculac

University of Split, Faculty of Science, Split, Croatia

Z. Antunovic, M. Kovac

Institute Rudjer Boskovic, Zagreb, Croatia

V. Brigljevic, D. Ferencek, K. Kadija, B. Mesic, M. Roguljic, A. Starodumov⁷, T. Susa

University of Cyprus, Nicosia, Cyprus

M.W. Ather, A. Attikis, M. Kolosova, G. Mavromanolakis, J. Mousa, C. Nicolaou, F. Ptochos, P.A. Razis, H. Rykaczewski

Charles University, Prague, Czech Republic

M. Finger⁸, M. Finger Jr.⁸

Escuela Politecnica Nacional, Quito, Ecuador

E. Ayala

Universidad San Francisco de Quito, Quito, Ecuador

E. Carrera Jarrin

**Academy of Scientific Research and Technology of the Arab Republic of Egypt,
Egyptian Network of High Energy Physics, Cairo, Egypt**

Y. Assran^{9,10}, S. Elgammal¹⁰, S. Khalil¹¹

National Institute of Chemical Physics and Biophysics, Tallinn, Estonia

S. Bhowmik, A. Carvalho Antunes De Oliveira, R.K. Dewanjee, K. Ehataht, M. Kadastik,
M. Raidal, C. Veelken

Department of Physics, University of Helsinki, Helsinki, Finland

P. Eerola, H. Kirschenmann, J. Pekkanen, M. Voutilainen

Helsinki Institute of Physics, Helsinki, Finland

J. Havukainen, J.K. Heikkilä, T. Järvinen, V. Karimäki, R. Kinnunen, T. Lampén,
K. Lassila-Perini, S. Laurila, S. Lehti, T. Lindén, P. Luukka, T. Mäenpää, H. Siikonen,
E. Tuominen, J. Tuominiemi

Lappeenranta University of Technology, Lappeenranta, Finland

T. Tuuva

IRFU, CEA, Université Paris-Saclay, Gif-sur-Yvette, France

M. Besancon, F. Couderc, M. Dejardin, D. Denegri, J.L. Faure, F. Ferri, S. Ganjour,
A. Givernaud, P. Gras, G. Hamel de Monchenault, P. Jarry, C. Leloup, E. Locci, J. Malcles,
G. Negro, J. Rander, A. Rosowsky, M.Ö. Sahin, M. Titov

**Laboratoire Leprince-Ringuet, Ecole polytechnique, CNRS/IN2P3, Université
Paris-Saclay, Palaiseau, France**

A. Abdulsalam¹², C. Amendola, I. Antropov, F. Beaudette, P. Busson, C. Charlot, B. Diab,
R. Granier de Cassagnac, I. Kucher, A. Lobanov, J. Martin Blanco, C. Martin Perez,
M. Nguyen, C. Ochando, G. Ortona, P. Paganini, J. Rembser, R. Salerno, J.B. Sauvan,
Y. Sirois, A.G. Stahl Leiton, A. Zabi, A. Zghiche

Université de Strasbourg, CNRS, IPHC UMR 7178, Strasbourg, France

J.-L. Agram¹³, J. Andrea, D. Bloch, G. Bourgatte, J.-M. Brom, E.C. Chabert,
V. Cherepanov, C. Collard, E. Conte¹³, J.-C. Fontaine¹³, D. Gelé, U. Goerlach, M. Jansová,
A.-C. Le Bihan, N. Tonon, P. Van Hove

**Centre de Calcul de l'Institut National de Physique Nucleaire et de Physique
des Particules, CNRS/IN2P3, Villeurbanne, France**

S. Gadrat

Université de Lyon, Université Claude Bernard Lyon 1, CNRS-IN2P3, Institut de Physique Nucléaire de Lyon, Villeurbanne, France

S. Beauceron, C. Bernet, G. Boudoul, N. Chanon, R. Chierici, D. Contardo, P. Depasse, H. El Mamouni, J. Fay, S. Gascon, M. Gouzevitch, G. Grenier, B. Ille, F. Lagarde, I.B. Laktineh, H. Lattaud, M. Lethuillier, L. Mirabito, S. Perries, A. Popov¹⁴, V. Sordini, G. Touquet, M. Vander Donckt, S. Viret

Georgian Technical University, Tbilisi, Georgia

A. Khvedelidze⁸

Tbilisi State University, Tbilisi, Georgia

Z. Tsamalaidze⁸

RWTH Aachen University, I. Physikalisches Institut, Aachen, Germany

C. Autermann, L. Feld, M.K. Kiesel, K. Klein, M. Lipinski, M. Preuten, M.P. Rauch, C. Schomakers, J. Schulz, M. Teroerde, B. Wittmer

RWTH Aachen University, III. Physikalisches Institut A, Aachen, Germany

A. Albert, M. Erdmann, S. Erdweg, T. Esch, R. Fischer, S. Ghosh, T. Hebbeker, C. Heidemann, K. Hoepfner, H. Keller, L. Mastrolorenzo, M. Merschmeyer, A. Meyer, P. Millet, S. Mukherjee, T. Pook, A. Pozdnyakov, M. Radziej, H. Reithler, M. Rieger, A. Schmidt, D. Teyssier, S. Thüer

RWTH Aachen University, III. Physikalisches Institut B, Aachen, Germany

G. Flügge, O. Hlushchenko, T. Kress, T. Müller, A. Nehr Korn, A. Nowack, C. Pistone, O. Pooth, D. Roy, H. Sert, A. Stahl¹⁵

Deutsches Elektronen-Synchrotron, Hamburg, Germany

M. Aldaya Martin, T. Arndt, C. Asawatangtrakuldee, I. Babounikau, K. Beernaert, O. Behnke, U. Behrens, A. Bermúdez Martínez, D. Bertsche, A.A. Bin Anuar, K. Borras¹⁶, V. Botta, A. Campbell, P. Connor, C. Contreras-Campana, V. Danilov, A. De Wit, M.M. Defranchis, C. Diez Pardos, D. Domínguez Damiani, G. Eckerlin, T. Eichhorn, A. Elwood, E. Eren, E. Gallo¹⁷, A. Geiser, J.M. Grados Luyando, A. Grohsjean, M. Guthoff, M. Haranko, A. Harb, H. Jung, M. Kasemann, J. Keaveney, C. Kleinwort, J. Knolle, D. Krücker, W. Lange, T. Lenz, J. Leonard, K. Lipka, W. Lohmann¹⁸, R. Mankel, I.-A. Melzer-Pellmann, A.B. Meyer, M. Meyer, M. Missiroli, G. Mittag, J. Mnich, V. Myronenko, S.K. Pflitsch, D. Pitzl, A. Raspereza, A. Saibel, M. Savitskyi, P. Saxena, P. Schütze, C. Schwanenberger, R. Shevchenko, A. Singh, H. Tholen, O. Turkot, A. Vagnerini, M. Van De Klundert, G.P. Van Onsem, R. Walsh, Y. Wen, K. Wichmann, C. Wissing, O. Zenaiev

University of Hamburg, Hamburg, Germany

R. Aggleton, S. Bein, L. Benato, A. Benecke, V. Blobel, T. Dreyer, A. Ebrahimi, E. Garutti, D. Gonzalez, P. Gunnellini, J. Haller, A. Hinzmann, A. Karavdina, G. Kasieczka, R. Klanner, R. Kogler, N. Kovalchuk, S. Kurz, V. Kutzner, J. Lange, D. Marconi, J. Multhaupt, M. Niedziela, C.E.N. Niemeyer, D. Nowatschin, A. Perieanu, A. Reimers, O. Rieger,

C. Scharf, P. Schleper, S. Schumann, J. Schwandt, J. Sonneveld, H. Stadie, G. Steinbrück, F.M. Stober, M. Stöver, B. Vormwald, I. Zoi

Karlsruher Institut fuer Technologie, Karlsruhe, Germany

M. Akbiyik, C. Barth, M. Baselga, S. Baur, E. Butz, R. Caspart, T. Chwalek, F. Colombo, W. De Boer, A. Dierlamm, K. El Morabit, N. Faltermann, B. Freund, M. Giffels, M.A. Harrendorf, F. Hartmann¹⁵, S.M. Heindl, U. Husemann, I. Katkov¹⁴, S. Kudella, S. Mitra, M.U. Mozer, Th. Müller, M. Musich, M. Plagge, G. Quast, K. Rabbertz, M. Schröder, I. Shvetsov, H.J. Simonis, R. Ulrich, S. Wayand, M. Weber, T. Weiler, C. Wöhrmann, R. Wolf

Institute of Nuclear and Particle Physics (INPP), NCSR Demokritos, Aghia Paraskevi, Greece

G. Anagnostou, G. Daskalakis, T. Geralis, A. Kyriakis, D. Loukas, G. Paspalaki

National and Kapodistrian University of Athens, Athens, Greece

A. Agapitos, G. Karathanasis, P. Kontaxakis, A. Panagiotou, I. Papavergou, N. Saoulidou, K. Vellidis

National Technical University of Athens, Athens, Greece

G. Bakas, K. Kousouris, I. Papakrivopoulos, G. Tsipolitis

University of Ioánnina, Ioánnina, Greece

I. Evangelou, C. Foudas, P. Gianneios, P. Katsoulis, P. Kokkas, S. Mallios, N. Manthos, I. Papadopoulos, E. Paradas, J. Strologas, F.A. Triantis, D. Tsitsonis

MTA-ELTE Lendület CMS Particle and Nuclear Physics Group, Eötvös Loránd University, Budapest, Hungary

M. Bartók¹⁹, M. Csanad, N. Filipovic, P. Major, A. Mehta, M.I. Nagy, G. Pasztor, O. Surányi, G.I. Veres

Wigner Research Centre for Physics, Budapest, Hungary

G. Bencze, C. Hajdu, D. Horvath²⁰, Á. Hunyadi, F. Sikler, T.Á. Vámi, V. Veszpremi, G. Vesztergombi[†]

Institute of Nuclear Research ATOMKI, Debrecen, Hungary

N. Beni, S. Czellar, J. Karancki¹⁹, A. Makovec, J. Molnar, Z. Szillasi

Institute of Physics, University of Debrecen, Debrecen, Hungary

P. Raics, Z.L. Trocsanyi, B. Ujvari

Indian Institute of Science (IISc), Bangalore, India

S. Choudhury, J.R. Komaragiri, P.C. Tiwari

National Institute of Science Education and Research, HBNI, Bhubaneswar, India

S. Bahinipati²², C. Kar, P. Mal, K. Mandal, A. Nayak²³, S. Roy Chowdhury, D.K. Sahoo²², S.K. Swain

Panjab University, Chandigarh, India

S. Bansal, S.B. Beri, V. Bhatnagar, S. Chauhan, R. Chawla, N. Dhingra, R. Gupta, A. Kaur, M. Kaur, S. Kaur, P. Kumari, M. Lohan, M. Meena, K. Sandeep, S. Sharma, J.B. Singh, A.K. Viridi, G. Walia

University of Delhi, Delhi, India

A. Bhardwaj, B.C. Choudhary, R.B. Garg, M. Gola, S. Keshri, Ashok Kumar, S. Malhotra, M. Naimuddin, P. Priyanka, K. Ranjan, Aashaq Shah, R. Sharma

Saha Institute of Nuclear Physics, HBNI, Kolkata, India

R. Bhardwaj²⁴, M. Bharti²⁴, R. Bhattacharya, S. Bhattacharya, U. Bhawandeep²⁴, D. Bhowmik, S. Dey, S. Dutt²⁴, S. Dutta, S. Ghosh, M. Maity²⁵, K. Mondal, S. Nandan, A. Purohit, P.K. Rout, A. Roy, G. Saha, S. Sarkar, T. Sarkar²⁵, M. Sharan, B. Singh²⁴, S. Thakur²⁴

Indian Institute of Technology Madras, Madras, India

P.K. Behera, A. Muhammad

Bhabha Atomic Research Centre, Mumbai, India

R. Chudasama, D. Dutta, V. Jha, V. Kumar, D.K. Mishra, P.K. Netrakanti, L.M. Pant, P. Shukla, P. Suggisetti

Tata Institute of Fundamental Research-A, Mumbai, India

T. Aziz, M.A. Bhat, S. Dugad, G.B. Mohanty, N. Sur, RavindraKumar Verma

Tata Institute of Fundamental Research-B, Mumbai, India

S. Banerjee, S. Bhattacharya, S. Chatterjee, P. Das, M. Guchait, Sa. Jain, S. Karmakar, S. Kumar, G. Majumder, K. Mazumdar, N. Sahoo

Indian Institute of Science Education and Research (IISER), Pune, India

S. Chauhan, S. Dube, V. Hegde, A. Kapoor, K. Kotheekar, S. Pandey, A. Rane, A. Rastogi, S. Sharma

Institute for Research in Fundamental Sciences (IPM), Tehran, Iran

S. Chenarani²⁶, E. Eskandari Tadavani, S.M. Etesami²⁶, M. Khakzad, M. Mohammadi Najafabadi, M. Naseri, F. Rezaei Hosseinabadi, B. Safarzadeh²⁷, M. Zeinali

University College Dublin, Dublin, Ireland

M. Felcini, M. Grunewald

INFN Sezione di Bari^a, Università di Bari^b, Politecnico di Bari^c, Bari, Italy

M. Abbrescia^{a,b}, C. Calabria^{a,b}, A. Colaleo^a, D. Creanza^{a,c}, L. Cristella^{a,b}, N. De Filippis^{a,c}, M. De Palma^{a,b}, A. Di Florio^{a,b}, F. Errico^{a,b}, L. Fiore^a, A. Gelmi^{a,b}, G. Iaselli^{a,c}, M. Ince^{a,b}, S. Lezki^{a,b}, G. Maggi^{a,c}, M. Maggi^a, G. Miniello^{a,b}, S. My^{a,b}, S. Nuzzo^{a,b}, A. Pompili^{a,b}, G. Pugliese^{a,c}, R. Radogna^a, A. Ranieri^a, G. Selvaggi^{a,b}, A. Sharma^a, L. Silvestris^a, R. Venditti^a, P. Verwilligen^a

INFN Sezione di Bologna^a, Università di Bologna^b, Bologna, Italy

G. Abbiendi^a, C. Battilana^{a,b}, D. Bonacorsi^{a,b}, L. Borghonovi^{a,b}, S. Braibant-Giacomelli^{a,b}, R. Campanini^{a,b}, P. Capiluppi^{a,b}, A. Castro^{a,b}, F.R. Cavallo^a, S.S. Chhibra^{a,b}, G. Codispoti^{a,b}, M. Cuffiani^{a,b}, G.M. Dallavalle^a, F. Fabbri^a, A. Fanfani^{a,b}, E. Fontanesi, P. Giacomelli^a, C. Grandi^a, L. Guiducci^{a,b}, F. Iemmi^{a,b}, S. Lo Meo^{a,28}, S. Marcellini^a, G. Masetti^a, A. Montanari^a, F.L. Navarria^{a,b}, A. Perrotta^a, F. Primavera^{a,b}, A.M. Rossi^{a,b}, T. Rovelli^{a,b}, G.P. Siroli^{a,b}, N. Tosi^a

INFN Sezione di Catania^a, Università di Catania^b, Catania, Italy

S. Albergò^{a,b,29}, A. Di Mattia^a, R. Potenza^{a,b}, A. Tricomi^{a,b,29}, C. Tuve^{a,b}

INFN Sezione di Firenze^a, Università di Firenze^b, Firenze, Italy

G. Barbagli^a, K. Chatterjee^{a,b}, V. Ciulli^{a,b}, C. Civinini^a, R. D'Alessandro^{a,b}, E. Focardi^{a,b}, G. Latino, P. Lenzi^{a,b}, M. Meschini^a, S. Paoletti^a, L. Russo^{a,30}, G. Sguazzoni^a, D. Strom^a, L. Viliani^a

INFN Laboratori Nazionali di Frascati, Frascati, Italy

L. Benussi, S. Bianco, F. Fabbri, D. Piccolo

INFN Sezione di Genova^a, Università di Genova^b, Genova, Italy

F. Ferro^a, R. Mulargia^{a,b}, E. Robutti^a, S. Tosi^{a,b}

INFN Sezione di Milano-Bicocca^a, Università di Milano-Bicocca^b, Milano, Italy

A. Benaglia^a, A. Beschi^b, F. Brivio^{a,b}, V. Ciriolo^{a,b,15}, S. Di Guida^{a,b,15}, M.E. Dinardo^{a,b}, S. Fiorendi^{a,b}, S. Gennai^a, A. Ghezzi^{a,b}, P. Govoni^{a,b}, M. Malberti^{a,b}, S. Malvezzi^a, D. Menasce^a, F. Monti, L. Moroni^a, M. Paganoni^{a,b}, D. Pedrini^a, S. Ragazzi^{a,b}, T. Tabarelli de Fatis^{a,b}, D. Zuolo^{a,b}

INFN Sezione di Napoli^a, Università di Napoli 'Federico II'^b, Napoli, Italy, Università della Basilicata^c, Potenza, Italy, Università G. Marconi^d, Roma, Italy

S. Buontempo^a, N. Cavallo^{a,c}, A. De Iorio^{a,b}, A. Di Crescenzo^{a,b}, F. Fabozzi^{a,c}, F. Fienga^a, G. Galati^a, A.O.M. Iorio^{a,b}, L. Lista^a, S. Meola^{a,d,15}, P. Paolucci^{a,15}, C. Sciacca^{a,b}, E. Voevodina^{a,b}

INFN Sezione di Padova^a, Università di Padova^b, Padova, Italy, Università di Trento^c, Trento, Italy

P. Azzi^a, N. Bacchetta^a, D. Bisello^{a,b}, A. Boletti^{a,b}, A. Bragagnolo, R. Carlin^{a,b}, P. Checchia^a, M. Dall'Osso^{a,b}, P. De Castro Manzano^a, T. Dorigo^a, U. Dosselli^a, F. Gasparini^{a,b}, U. Gasparini^{a,b}, A. Gozzelino^a, S.Y. Hoh, S. Lacaprara^a, P. Lujan, M. Margoni^{a,b}, A.T. Meneguzzo^{a,b}, J. Pazzini^{a,b}, M. Presilla^b, P. Ronchese^{a,b}, R. Rossin^{a,b}, F. Simonetto^{a,b}, A. Tiko, E. Torassa^a, M. Tosi^{a,b}, M. Zanetti^{a,b}, P. Zotto^{a,b}, G. Zumerle^{a,b}

INFN Sezione di Pavia^a, Università di Pavia^b, Pavia, Italy

A. Braghieri^a, A. Magnani^a, P. Montagna^{a,b}, S.P. Ratti^{a,b}, V. Re^a, M. Ressegotti^{a,b}, C. Riccardi^{a,b}, P. Salvini^a, I. Vai^{a,b}, P. Vitulo^{a,b}

INFN Sezione di Perugia^a, Università di Perugia^b, Perugia, Italy

M. Biasini^{a,b}, G.M. Bilei^a, C. Cecchi^{a,b}, D. Ciangottini^{a,b}, L. Fanò^{a,b}, P. Lariccia^{a,b}, R. Leonardi^{a,b}, E. Manoni^a, G. Mantovani^{a,b}, V. Mariani^{a,b}, M. Menichelli^a, A. Rossi^{a,b}, A. Santocchia^{a,b}, D. Spiga^a

INFN Sezione di Pisa^a, Università di Pisa^b, Scuola Normale Superiore di Pisa^c, Pisa, Italy

K. Androsov^a, P. Azzurri^a, G. Bagliesi^a, L. Bianchini^a, T. Boccali^a, L. Borrello, R. Castaldi^a, M.A. Ciocci^{a,b}, R. Dell'Orso^a, G. Fedi^a, F. Fiori^{a,c}, L. Giannini^{a,c}, A. Giassi^a, M.T. Grippo^a, F. Ligabue^{a,c}, E. Manca^{a,c}, G. Mandorli^{a,c}, A. Messineo^{a,b}, F. Palla^a, A. Rizzi^{a,b}, G. Rolandi³¹, P. Spagnolo^a, R. Tenchini^a, G. Tonelli^{a,b}, A. Venturi^a, P.G. Verdini^a

INFN Sezione di Roma^a, Sapienza Università di Roma^b, Rome, Italy

L. Barone^{a,b}, F. Cavallari^a, M. Cipriani^{a,b}, D. Del Re^{a,b}, E. Di Marco^{a,b}, M. Diemmoz^a, S. Gelli^{a,b}, E. Longo^{a,b}, B. Marzocchi^{a,b}, P. Meridiani^a, G. Organtini^{a,b}, F. Pandolfi^a, R. Paramatti^{a,b}, F. Preiato^{a,b}, S. Rahatlou^{a,b}, C. Rovelli^a, F. Santanastasio^{a,b}

INFN Sezione di Torino^a, Università di Torino^b, Torino, Italy, Università del Piemonte Orientale^c, Novara, Italy

N. Amapane^{a,b}, R. Arcidiacono^{a,c}, S. Argiro^{a,b}, M. Arneodo^{a,c}, N. Bartosik^a, R. Bellan^{a,b}, C. Biino^a, A. Cappati^{a,b}, N. Cartiglia^a, F. Cenna^{a,b}, S. Cometti^a, M. Costa^{a,b}, R. Covarelli^{a,b}, N. Demaria^a, B. Kiani^{a,b}, C. Mariotti^a, S. Maselli^a, E. Migliore^{a,b}, V. Monaco^{a,b}, E. Monteil^{a,b}, M. Monteno^a, M.M. Obertino^{a,b}, L. Pacher^{a,b}, N. Pastrone^a, M. Pelliccioni^a, G.L. Pinna Angioni^{a,b}, A. Romero^{a,b}, M. Ruspa^{a,c}, R. Sacchi^{a,b}, R. Salvatico^{a,b}, K. Shchelina^{a,b}, V. Sola^a, A. Solano^{a,b}, D. Soldi^{a,b}, A. Staiano^a

INFN Sezione di Trieste^a, Università di Trieste^b, Trieste, Italy

S. Belforte^a, V. Candelise^{a,b}, M. Casarsa^a, F. Cossutti^a, A. Da Rold^{a,b}, G. Della Ricca^{a,b}, F. Vazzoler^{a,b}, A. Zanetti^a

Kyungpook National University, Daegu, Korea

D.H. Kim, G.N. Kim, M.S. Kim, J. Lee, S.W. Lee, C.S. Moon, Y.D. Oh, S.I. Pak, S. Sekmen, D.C. Son, Y.C. Yang

Chonnam National University, Institute for Universe and Elementary Particles, Kwangju, Korea

H. Kim, D.H. Moon, G. Oh

Hanyang University, Seoul, Korea

B. Francois, J. Goh³², T.J. Kim

Korea University, Seoul, Korea

S. Cho, S. Choi, Y. Go, D. Gyun, S. Ha, B. Hong, Y. Jo, K. Lee, K.S. Lee, S. Lee, J. Lim, S.K. Park, Y. Roh

Sejong University, Seoul, Korea

H.S. Kim

Seoul National University, Seoul, Korea

J. Almond, J. Kim, J.S. Kim, H. Lee, K. Lee, S. Lee, K. Nam, S.B. Oh, B.C. Radburn-Smith, S.h. Seo, U.K. Yang, H.D. Yoo, G.B. Yu

University of Seoul, Seoul, Korea

D. Jeon, H. Kim, J.H. Kim, J.S.H. Lee, I.C. Park

Sungkyunkwan University, Suwon, Korea

Y. Choi, C. Hwang, J. Lee, I. Yu

Riga Technical University, Riga, Latvia

V. Veckalns³³

Vilnius University, Vilnius, Lithuania

V. Dudenas, A. Juodagalvis, J. Vaitkus

National Centre for Particle Physics, Universiti Malaya, Kuala Lumpur, Malaysia

Z.A. Ibrahim, M.A.B. Md Ali³⁴, F. Mohamad Idris³⁵, W.A.T. Wan Abdullah, M.N. Yusli, Z. Zolkapli

Universidad de Sonora (UNISON), Hermosillo, Mexico

J.F. Benitez, A. Castaneda Hernandez, J.A. Murillo Quijada

Centro de Investigacion y de Estudios Avanzados del IPN, Mexico City, Mexico

H. Castilla-Valdez, E. De La Cruz-Burelo, M.C. Duran-Osuna, I. Heredia-De La Cruz³⁶, R. Lopez-Fernandez, J. Mejia Guisao, R.I. Rabadan-Trejo, M. Ramirez-Garcia, G. Ramirez-Sanchez, R. Reyes-Almanza, A. Sanchez-Hernandez

Universidad Iberoamericana, Mexico City, Mexico

S. Carrillo Moreno, C. Oropeza Barrera, F. Vazquez Valencia

Benemerita Universidad Autonoma de Puebla, Puebla, Mexico

J. Eysermans, I. Pedraza, H.A. Salazar Ibarquen, C. Uribe Estrada

Universidad Autónoma de San Luis Potosí, San Luis Potosí, Mexico

A. Morelos Pineda

University of Auckland, Auckland, New Zealand

D. Krofcheck

University of Canterbury, Christchurch, New Zealand

S. Bheesette, P.H. Butler

National Centre for Physics, Quaid-I-Azam University, Islamabad, Pakistan

A. Ahmad, M. Ahmad, M.I. Asghar, Q. Hassan, H.R. Hoorani, W.A. Khan, M.A. Shah, M. Shoaib, M. Waqas

National Centre for Nuclear Research, Swierk, Poland

H. Bialkowska, M. Bluj, B. Boimska, T. Frueboes, M. Górski, M. Kazana, M. Szeleper, P. Traczyk, P. Zalewski

Institute of Experimental Physics, Faculty of Physics, University of Warsaw, Warsaw, Poland

K. Bunkowski, A. Byszuk³⁷, K. Doroba, A. Kalinowski, M. Konecki, J. Krolikowski, M. Misiura, M. Olszewski, A. Pyskir, M. Walczak

Laboratório de Instrumentação e Física Experimental de Partículas, Lisboa, Portugal

M. Araujo, P. Bargassa, C. Beirão Da Cruz E Silva, A. Di Francesco, P. Faccioli, B. Galinhas, M. Gallinaro, J. Hollar, N. Leonardo, J. Seixas, G. Strong, O. Toldaiev, J. Varela

Joint Institute for Nuclear Research, Dubna, Russia

S. Afanasiev, P. Bunin, M. Gavrilenko, I. Golutvin, I. Gorbunov, A. Kamenev, V. Karjavine, A. Lanev, A. Malakhov, V. Matveev^{38,39}, P. Moisev, V. Palichik, V. Perelygin, S. Shmatov, S. Shulha, N. Skatchkov, V. Smirnov, N. Voytishin, A. Zarubin

Petersburg Nuclear Physics Institute, Gatchina (St. Petersburg), Russia

V. Golovtsov, Y. Ivanov, V. Kim⁴⁰, E. Kuznetsova⁴¹, P. Levchenko, V. Murzin, V. Oreshkin, I. Smirnov, D. Sosnov, V. Sulimov, L. Uvarov, S. Vavilov, A. Vorobyev

Institute for Nuclear Research, Moscow, Russia

Yu. Andreev, A. Dermenev, S. Gninenko, N. Golubev, A. Karneyev, M. Kirsanov, N. Krasnikov, A. Pashenkov, A. Shabanov, D. Tlisov, A. Toropin

Institute for Theoretical and Experimental Physics named by A.I. Alikhanov of NRC ‘Kurchatov Institute’, Moscow, Russia

V. Epshteyn, V. Gavrillov, N. Lychkovskaya, V. Popov, I. Pozdnyakov, G. Safronov, A. Spiridonov, A. Stepenov, V. Stolin, M. Toms, E. Vlasov, A. Zhokin

Moscow Institute of Physics and Technology, Moscow, Russia

T. Aushev

National Research Nuclear University ‘Moscow Engineering Physics Institute’ (MEPhI), Moscow, Russia

R. Chistov⁴², M. Danilov⁴², P. Parygin, E. Tarkovskii

P.N. Lebedev Physical Institute, Moscow, Russia

V. Andreev, M. Azarkin, I. Dremin³⁹, M. Kirakosyan, A. Terkulov

Skobeltsyn Institute of Nuclear Physics, Lomonosov Moscow State University, Moscow, Russia

A. Belyaev, E. Boos, M. Dubinin⁴³, L. Dudko, A. Ershov, A. Gribushin, V. Klyukhin, O. Kodolova, I. Lokhtin, S. Obraztsov, S. Petrushanko, V. Savrin, A. Snigirev

Novosibirsk State University (NSU), Novosibirsk, Russia

A. Barnyakov⁴⁴, V. Blinov⁴⁴, T. Dimova⁴⁴, L. Kardapoltsev⁴⁴, Y. Skovpen⁴⁴

Institute for High Energy Physics of National Research Centre ‘Kurchatov Institute’, Protvino, Russia

I. Azhgirey, I. Bayshev, S. Bitioukov, V. Kachanov, A. Kalinin, D. Konstantinov, P. Mandrik, V. Petrov, R. Ryutin, S. Slabospitskii, A. Sobol, S. Troshin, N. Tyurin, A. Uzunian, A. Volkov

National Research Tomsk Polytechnic University, Tomsk, Russia

A. Babaev, S. Baidali, V. Okhotnikov

University of Belgrade: Faculty of Physics and VINCA Institute of Nuclear Sciences

P. Adzic⁴⁵, P. Cirkovic, D. Devetak, M. Dordevic, P. Milenovic⁴⁶, J. Milosevic

Centro de Investigaciones Energéticas Medioambientales y Tecnológicas (CIEMAT), Madrid, Spain

J. Alcaraz Maestre, A. Álvarez Fernández, I. Bachiller, M. Barrio Luna, J.A. Brochero Cifuentes, M. Cerrada, N. Colino, B. De La Cruz, A. Delgado Peris, C. Fernandez Bedoya, J.P. Fernández Ramos, J. Flix, M.C. Fouz, O. Gonzalez Lopez, S. Goy Lopez, J.M. Hernandez, M.I. Josa, D. Moran, A. Pérez-Calero Yzquierdo, J. Puerta Pelayo, I. Redondo, L. Romero, S. Sánchez Navas, M.S. Soares, A. Triossi

Universidad Autónoma de Madrid, Madrid, Spain

C. Albajar, J.F. de Trocóniz

Universidad de Oviedo, Oviedo, Spain

J. Cuevas, C. Erice, J. Fernandez Menendez, S. Folgueras, I. Gonzalez Caballero, J.R. González Fernández, E. Palencia Cortezon, V. Rodríguez Bouza, S. Sanchez Cruz, J.M. Vizán García

Instituto de Física de Cantabria (IFCA), CSIC-Universidad de Cantabria, Santander, Spain

I.J. Cabrillo, A. Calderon, B. Chazin Quero, J. Duarte Campderros, M. Fernandez, P.J. Fernández Manteca, A. García Alonso, J. Garcia-Ferrero, G. Gomez, A. Lopez Virto, J. Marco, C. Martinez Rivero, P. Martinez Ruiz del Arbol, F. Matorras, J. Piedra Gomez, C. Prieels, T. Rodrigo, A. Ruiz-Jimeno, L. Scodellaro, N. Trevisani, I. Vila, R. Villar Cortabitarte

University of Ruhuna, Department of Physics, Matara, Sri Lanka

N. Wickramage

CERN, European Organization for Nuclear Research, Geneva, Switzerland

D. Abbaneo, B. Akgun, E. Auffray, G. Auzinger, P. Baillon, A.H. Ball, D. Barney, J. Bendavid, M. Bianco, A. Bocci, C. Botta, E. Brondolin, T. Camporesi, M. Cepeda, G. Cerminara, E. Chapon, Y. Chen, G. Cucciati, D. d’Enterria, A. Dabrowski, N. Daci, V. Daponte, A. David, A. De Roeck, N. Deelen, M. Dobson, M. Dünser, N. Dupont, A. Elliott-Peisert, F. Fallavollita⁴⁷, D. Fasanella, G. Franzoni, J. Fulcher, W. Funk, D. Gigi, A. Gilbert, K. Gill, F. Glege, M. Gruchala, M. Guilbaud, D. Gulhan, J. Hegeman, C. Heidegger,

Y. Iiyama, V. Innocente, G.M. Innocenti, A. Jafari, P. Janot, O. Karacheban¹⁸, J. Kieseler, A. Kornmayer, M. Krammer¹, C. Lange, P. Lecoq, C. Lourenço, L. Malgeri, M. Mannelli, A. Massironi, F. Meijers, J.A. Merlin, S. Mersi, E. Meschi, F. Moortgat, M. Mulders, J. Ngadiuba, S. Nourbakhsh, S. Orfanelli, L. Orsini, F. Pantaleo¹⁵, L. Pape, E. Perez, M. Peruzzi, A. Petrilli, G. Petrucciani, A. Pfeiffer, M. Pierini, F.M. Pitters, D. Rabaday, A. Racz, M. Rovere, H. Sakulin, C. Schäfer, C. Schwick, M. Selvaggi, A. Sharma, P. Silva, P. Sphicas⁴⁸, A. Stakia, J. Steggemann, D. Treille, A. Tsirou, A. Vartak, M. Verzetti, W.D. Zeuner

Paul Scherrer Institut, Villigen, Switzerland

L. Caminada⁴⁹, K. Deiters, W. Erdmann, R. Horisberger, Q. Ingram, H.C. Kaestli, D. Kotlinski, U. Langenegger, T. Rohe, S.A. Wiederkehr

ETH Zurich — Institute for Particle Physics and Astrophysics (IPA), Zurich, Switzerland

M. Backhaus, L. Bäni, P. Berger, N. Chernyavskaya, G. Dissertori, M. Dittmar, M. Donegà, C. Dorfer, T.A. Gómez Espinosa, C. Grab, D. Hits, T. Klijnsma, W. Luster, R.A. Manzoni, M. Marionneau, M.T. Meinhard, F. Micheli, P. Musella, F. Nessi-Tedaldi, F. Pauss, G. Perrin, L. Perrozzi, S. Pigazzini, M. Reichmann, C. Reissel, D. Ruini, D.A. Sanz Becerra, M. Schönenberger, L. Shchutska, V.R. Tavolaro, K. Theofilatos, M.L. Vesterbacka Olsson, R. Wallny, D.H. Zhu

Universität Zürich, Zurich, Switzerland

T.K. Aarrestad, C. Amsler⁵⁰, D. Brzhechko, M.F. Canelli, A. De Cosa, R. Del Burgo, S. Donato, C. Galloni, T. Hreus, B. Kilminster, S. Leontsinis, V.M. Mikuni, I. Neutelings, G. Rauco, P. Robmann, D. Salerno, K. Schweiger, C. Seitz, Y. Takahashi, S. Wertz, A. Zucchetta

National Central University, Chung-Li, Taiwan

T.H. Doan, C.M. Kuo, W. Lin, S.S. Yu

National Taiwan University (NTU), Taipei, Taiwan

P. Chang, Y. Chao, K.F. Chen, P.H. Chen, W.-S. Hou, Y.F. Liu, R.-S. Lu, E. Paganis, A. Psallidas, A. Steen

Chulalongkorn University, Faculty of Science, Department of Physics, Bangkok, Thailand

B. Asavapibhop, N. Srimanobhas, N. Suwonjandee

Çukurova University, Physics Department, Science and Art Faculty, Adana, Turkey

A. Bat, F. Boran, S. Cerci⁵¹, S. Damarseckin, Z.S. Demiroglu, F. Dolek, C. Dozen, I. Dumanoglu, G. Gokbulut, EmineGurpinar Guler⁵², Y. Guler, I. Hos⁵³, C. Isik, E.E. Kangal⁵⁴, O. Kara, U. Kiminsu, M. Oglakci, G. Onengut, K. Ozdemir⁵⁵, S. Ozturk⁵⁶, A. Polatoz, D. Sunar Cerci⁵¹, B. Tali⁵¹, U.G. Tok, S. Turkcapar, I.S. Zorbakir, C. Zorbilmez

Middle East Technical University, Physics Department, Ankara, Turkey

B. Isildak⁵⁷, G. Karapinar⁵⁸, M. Yalvac, M. Zeyrek

Bogazici University, Istanbul, Turkey

I.O. Atakisi, E. Gülmez, M. Kaya⁵⁹, O. Kaya⁶⁰, Ö. Özçelik, S. Ozkorucuklu⁶¹, S. Tekten, E.A. Yetkin⁶²

Istanbul Technical University, Istanbul, Turkey

M.N. Agaras, A. Cakir, K. Cankocak, Y. Komurcu, S. Sen⁶³

Institute for Scintillation Materials of National Academy of Science of Ukraine, Kharkov, Ukraine

B. Grynyov

National Scientific Center, Kharkov Institute of Physics and Technology, Kharkov, Ukraine

L. Levchuk

University of Bristol, Bristol, United Kingdom

F. Ball, J.J. Brooke, D. Burns, E. Clement, D. Cussans, O. Davignon, H. Flacher, J. Goldstein, G.P. Heath, H.F. Heath, L. Kreczko, D.M. Newbold⁶⁴, S. Paramesvaran, B. Penning, T. Sakuma, D. Smith, V.J. Smith, J. Taylor, A. Titterton

Rutherford Appleton Laboratory, Didcot, United Kingdom

K.W. Bell, A. Belyaev⁶⁵, C. Brew, R.M. Brown, D. Cieri, D.J.A. Cockerill, J.A. Coughlan, K. Harder, S. Harper, J. Linacre, K. Manolopoulos, E. Olaiya, D. Petyt, T. Reis, T. Schuh, C.H. Shepherd-Themistocleous, A. Thea, I.R. Tomalin, T. Williams, W.J. Womersley

Imperial College, London, United Kingdom

R. Bainbridge, P. Bloch, J. Borg, S. Breeze, O. Buchmuller, A. Bundock, D. Colling, P. Dauncey, G. Davies, M. Della Negra, R. Di Maria, P. Everaerts, G. Hall, G. Iles, T. James, M. Komm, C. Laner, L. Lyons, A.-M. Magnan, S. Malik, A. Martelli, J. Nash⁶⁶, A. Nikitenko⁷, V. Palladino, M. Pesaresi, D.M. Raymond, A. Richards, A. Rose, E. Scott, C. Seez, A. Shtipliyski, G. Singh, M. Stoye, T. Strebler, S. Summers, A. Tapper, K. Uchida, T. Virdee¹⁵, N. Wardle, D. Winterbottom, J. Wright, S.C. Zenz

Brunel University, Uxbridge, United Kingdom

J.E. Cole, P.R. Hobson, A. Khan, P. Kyberd, C.K. Mackay, A. Morton, I.D. Reid, L. Teodorescu, S. Zahid

Baylor University, Waco, U.S.A.

K. Call, J. Dittmann, K. Hatakeyama, H. Liu, C. Madrid, B. McMaster, N. Pastika, C. Smith

Catholic University of America, Washington, DC, U.S.A.

R. Bartek, A. Dominguez

The University of Alabama, Tuscaloosa, U.S.A.

A. Buccilli, O. Charaf, S.I. Cooper, C. Henderson, P. Rumerio, C. West

Boston University, Boston, U.S.A.

D. Arcaro, T. Bose, Z. Demiragli, D. Gastler, S. Girgis, D. Pinna, C. Richardson, J. Rohlf, D. Sperka, I. Suarez, L. Sulak, D. Zou

Brown University, Providence, U.S.A.

G. Benelli, B. Burkle, X. Coubez, D. Cutts, M. Hadley, J. Hakala, U. Heintz, J.M. Hogan⁶⁷, K.H.M. Kwok, E. Laird, G. Landsberg, J. Lee, Z. Mao, M. Narain, S. Sagir⁶⁸, R. Syarif, E. Usai, D. Yu

University of California, Davis, Davis, U.S.A.

R. Band, C. Brainerd, R. Breedon, D. Burns, M. Calderon De La Barca Sanchez, M. Chertok, J. Conway, R. Conway, P.T. Cox, R. Erbacher, C. Flores, G. Funk, W. Ko, O. Kukral, R. Lander, M. Mulhearn, D. Pellett, J. Pilot, S. Shalhout, M. Shi, D. Stolp, D. Taylor, K. Tos, M. Tripathi, Z. Wang, F. Zhang

University of California, Los Angeles, U.S.A.

M. Bachtis, C. Bravo, R. Cousins, A. Dasgupta, A. Florent, J. Hauser, M. Ignatenko, N. Mccoll, S. Regnard, D. Saltzberg, C. Schnaible, V. Valuev

University of California, Riverside, Riverside, U.S.A.

E. Bouvier, K. Burt, R. Clare, J.W. Gary, S.M.A. Ghiasi Shirazi, G. Hanson, G. Karapostoli, E. Kennedy, F. Lacroix, O.R. Long, M. Olmedo Negrete, M.I. Paneva, W. Si, L. Wang, H. Wei, S. Wimpenny, B.R. Yates

University of California, San Diego, La Jolla, U.S.A.

J.G. Branson, P. Chang, S. Cittolin, M. Derdzinski, R. Gerosa, D. Gilbert, B. Hashemi, A. Holzner, D. Klein, G. Kole, V. Krutelyov, J. Letts, M. Masciovecchio, S. May, D. Olivito, S. Padhi, M. Pieri, V. Sharma, M. Tadel, J. Wood, F. Würthwein, A. Yagil, G. Zevi Della Porta

University of California, Santa Barbara — Department of Physics, Santa Barbara, U.S.A.

N. Amin, R. Bhandari, C. Campagnari, M. Citron, V. Dutta, M. Franco Sevilla, L. Gouskos, R. Heller, J. Incandela, H. Mei, A. Ovcharova, H. Qu, J. Richman, D. Stuart, S. Wang, J. Yoo

California Institute of Technology, Pasadena, U.S.A.

D. Anderson, A. Bornheim, J.M. Lawhorn, N. Lu, H.B. Newman, T.Q. Nguyen, J. Pata, M. Spiropulu, J.R. Vlimant, R. Wilkinson, S. Xie, Z. Zhang, R.Y. Zhu

Carnegie Mellon University, Pittsburgh, U.S.A.

M.B. Andrews, T. Ferguson, T. Mudholkar, M. Paulini, M. Sun, I. Vorobiev, M. Weinberg

University of Colorado Boulder, Boulder, U.S.A.

J.P. Cumalat, W.T. Ford, F. Jensen, A. Johnson, E. MacDonald, T. Mulholland, R. Patel, A. Perloff, K. Stenson, K.A. Ulmer, S.R. Wagner

Cornell University, Ithaca, U.S.A.

J. Alexander, J. Chaves, Y. Cheng, J. Chu, A. Datta, K. McDermott, N. Mirman, J. Monroy, J.R. Patterson, D. Quach, A. Rinkevicius, A. Ryd, L. Skinnari, L. Soffi, S.M. Tan, Z. Tao, J. Thom, J. Tucker, P. Wittich, M. Zientek

Fermi National Accelerator Laboratory, Batavia, U.S.A.

S. Abdullin, M. Albrow, M. Alyari, G. Apollinari, A. Apresyan, A. Apyan, S. Banerjee, L.A.T. Bauerdick, A. Beretvas, J. Berryhill, P.C. Bhat, K. Burkett, J.N. Butler, A. Canepa, G.B. Cerati, H.W.K. Cheung, F. Chlebana, M. Cremonesi, J. Duarte, V.D. Elvira, J. Freeman, Z. Gecse, E. Gottschalk, L. Gray, D. Green, S. Grünendahl, O. Gutsche, J. Hanlon, R.M. Harris, S. Hasegawa, J. Hirschauer, Z. Hu, B. Jayatilaka, S. Jindariani, M. Johnson, U. Joshi, B. Klima, M.J. Kortelainen, B. Kreis, S. Lammel, D. Lincoln, R. Lipton, M. Liu, T. Liu, J. Lykken, K. Maeshima, J.M. Marraffino, D. Mason, P. McBride, P. Merkel, S. Mrenna, S. Nahn, V. O'Dell, K. Pedro, C. Pena, O. Prokofyev, G. Rakness, F. Ravera, A. Reinsvold, L. Ristori, A. Savoy-Navarro⁶⁹, B. Schneider, E. Sexton-Kennedy, A. Soha, W.J. Spalding, L. Spiegel, S. Stoynev, J. Strait, N. Strobbe, L. Taylor, S. Tkaczyk, N.V. Tran, L. Uplegger, E.W. Vaandering, C. Vernieri, M. Verzocchi, R. Vidal, M. Wang, H.A. Weber

University of Florida, Gainesville, U.S.A.

D. Acosta, P. Avery, P. Bortignon, D. Bourilkov, A. Brinkerhoff, L. Cadamuro, A. Carnes, D. Curry, R.D. Field, S.V. Gleyzer, B.M. Joshi, J. Konigsberg, A. Korytov, K.H. Lo, P. Ma, K. Matchev, N. Menendez, G. Mitselmakher, D. Rosenzweig, K. Shi, J. Wang, S. Wang, X. Zuo

Florida International University, Miami, U.S.A.

Y.R. Joshi, S. Linn

Florida State University, Tallahassee, U.S.A.

A. Ackert, T. Adams, A. Askew, S. Hagopian, V. Hagopian, K.F. Johnson, R. Khurana, T. Kolberg, G. Martinez, T. Perry, H. Prosper, A. Saha, C. Schiber, R. Yohay

Florida Institute of Technology, Melbourne, U.S.A.

M.M. Baarmand, V. Bhopatkar, S. Colafranceschi, M. Hohlmann, D. Noonan, M. Rahmani, T. Roy, M. Saunders, F. Yumiceva

University of Illinois at Chicago (UIC), Chicago, U.S.A.

M.R. Adams, L. Apanasevich, D. Berry, R.R. Betts, R. Cavanaugh, X. Chen, S. Dittmer, O. Evdokimov, C.E. Gerber, D.A. Hangal, D.J. Hofman, K. Jung, J. Kamin, C. Mills, M.B. Tonjes, N. Varelas, H. Wang, X. Wang, Z. Wu, J. Zhang

The University of Iowa, Iowa City, U.S.A.

M. Alhusseini, B. Bilki⁵², W. Clarida, K. Dilsiz⁷⁰, S. Durgut, R.P. Gandrajula, M. Haytmyradov, V. Khristenko, J.-P. Merlo, A. Mestvirishvili, A. Moeller, J. Nachtman, H. Ogul⁷¹, Y. Onel, F. Ozok⁷², A. Penzo, C. Snyder, E. Tiras, J. Wetzel

Johns Hopkins University, Baltimore, U.S.A.

B. Blumenfeld, A. Cocoros, N. Eminizer, D. Fehling, L. Feng, A.V. Gritsan, W.T. Hung, P. Maksimovic, J. Roskes, U. Sarica, M. Swartz, M. Xiao

The University of Kansas, Lawrence, U.S.A.

A. Al-bataineh, P. Baringer, A. Bean, S. Boren, J. Bowen, A. Bylinkin, J. Castle, S. Khalil, A. Kropivnitskaya, D. Majumder, W. Mcbrayer, M. Murray, C. Rogan, S. Sanders, E. Schmitz, J.D. Tapia Takaki, Q. Wang

Kansas State University, Manhattan, U.S.A.

S. Duric, A. Ivanov, K. Kaadze, D. Kim, Y. Maravin, D.R. Mendis, T. Mitchell, A. Modak, A. Mohammadi

Lawrence Livermore National Laboratory, Livermore, U.S.A.

F. Rebassoo, D. Wright

University of Maryland, College Park, U.S.A.

A. Baden, O. Baron, A. Belloni, S.C. Eno, Y. Feng, C. Ferraioli, N.J. Hadley, S. Jabeen, G.Y. Jeng, R.G. Kellogg, J. Kunkle, A.C. Mignerey, S. Nabili, F. Ricci-Tam, M. Seidel, Y.H. Shin, A. Skuja, S.C. Tonwar, K. Wong

Massachusetts Institute of Technology, Cambridge, U.S.A.

D. Abercrombie, B. Allen, V. Azzolini, A. Baty, R. Bi, S. Brandt, W. Busza, I.A. Cali, M. D'Alfonso, G. Gomez Ceballos, M. Goncharov, P. Harris, D. Hsu, M. Hu, M. Klute, D. Kovalskyi, Y.-J. Lee, P.D. Luckey, B. Maier, A.C. Marini, C. McGinn, C. Mironov, S. Narayanan, X. Niu, C. Paus, D. Rankin, C. Roland, G. Roland, Z. Shi, G.S.F. Stephans, K. Sumorok, K. Tatar, D. Velicanu, J. Wang, T.W. Wang, B. Wyslouch

University of Minnesota, Minneapolis, U.S.A.

A.C. Benvenuti[†], R.M. Chatterjee, A. Evans, P. Hansen, J. Hiltbrand, Sh. Jain, S. Kalafut, M. Krohn, Y. Kubota, Z. Lesko, J. Mans, R. Rusack, M.A. Wadud

University of Mississippi, Oxford, U.S.A.

J.G. Acosta, S. Oliveros

University of Nebraska-Lincoln, Lincoln, U.S.A.

E. Avdeeva, K. Bloom, D.R. Claes, C. Fangmeier, L. Finco, F. Golf, R. Gonzalez Suarez, R. Kamalieddin, I. Kravchenko, J.E. Siado, G.R. Snow, B. Stieger

State University of New York at Buffalo, Buffalo, U.S.A.

A. Godshalk, C. Harrington, I. Iashvili, A. Kharchilava, C. Mclean, D. Nguyen, A. Parker, S. Rappoccio, B. Roozbahani

Northeastern University, Boston, U.S.A.

G. Alverson, E. Barberis, C. Freer, Y. Haddad, A. Hortiangtham, G. Madigan, D.M. Morse, T. Orimoto, A. Tishelman-charny, T. Wamorkar, B. Wang, A. Wisecarver, D. Wood

Northwestern University, Evanston, U.S.A.

S. Bhattacharya, J. Bueghly, T. Gunter, K.A. Hahn, N. Odell, M.H. Schmitt, K. Sung, M. Trovato, M. Velasco

University of Notre Dame, Notre Dame, U.S.A.

R. Bucci, N. Dev, R. Goldouzian, M. Hildreth, K. Hurtado Anampa, C. Jessop, D.J. Karmgard, K. Lannon, W. Li, N. Loukas, N. Marinelli, F. Meng, C. Mueller, Y. Musienko³⁸, M. Planer, R. Ruchti, P. Siddireddy, G. Smith, S. Taroni, M. Wayne, A. Wightman, M. Wolf, A. Woodard

The Ohio State University, Columbus, U.S.A.

J. Alimena, L. Antonelli, B. Bylsma, L.S. Durkin, S. Flowers, B. Francis, C. Hill, W. Ji, A. Lefeld, T.Y. Ling, W. Luo, B.L. Winer

Princeton University, Princeton, U.S.A.

S. Cooperstein, G. Dezoort, P. Elmer, J. Hardenbrook, N. Haubrich, S. Higginbotham, A. Kalogeropoulos, S. Kwan, D. Lange, M.T. Lucchini, J. Luo, D. Marlow, K. Mei, I. Ojalvo, J. Olsen, C. Palmer, P. Piroué, J. Salfeld-Nebgen, D. Stickland, C. Tully

University of Puerto Rico, Mayaguez, U.S.A.

S. Malik, S. Norberg

Purdue University, West Lafayette, U.S.A.

A. Barker, V.E. Barnes, S. Das, L. Gutay, M. Jones, A.W. Jung, A. Khatiwada, B. Mahakud, D.H. Miller, N. Neumeister, C.C. Peng, S. Piperov, H. Qiu, J.F. Schulte, J. Sun, F. Wang, R. Xiao, W. Xie

Purdue University Northwest, Hammond, U.S.A.

T. Cheng, J. Dolen, N. Parashar

Rice University, Houston, U.S.A.

Z. Chen, K.M. Ecklund, S. Freed, F.J.M. Geurts, M. Kilpatrick, Arun Kumar, W. Li, B.P. Padley, R. Redjimi, J. Roberts, J. Rorie, W. Shi, Z. Tu, A. Zhang

University of Rochester, Rochester, U.S.A.

A. Bodek, P. de Barbaro, R. Demina, Y.t. Duh, J.L. Dulemba, C. Fallon, T. Ferbel, M. Galanti, A. Garcia-Bellido, J. Han, O. Hindrichs, A. Khukhunaishvili, E. Ranken, P. Tan, R. Taus

Rutgers, The State University of New Jersey, Piscataway, U.S.A.

B. Chiarito, J.P. Chou, Y. Gershtein, E. Halkiadakis, A. Hart, M. Heindl, E. Hughes, S. Kaplan, R. Kunnawalkam Elayavalli, S. Kyriacou, I. Laflotte, A. Lath, R. Montalvo, K. Nash, M. Osherson, H. Saka, S. Salur, S. Schnetzer, D. Sheffield, S. Somalwar, R. Stone, S. Thomas, P. Thomassen

University of Tennessee, Knoxville, U.S.A.

H. Acharya, A.G. Delannoy, J. Heideman, G. Riley, S. Spanier

Texas A&M University, College Station, U.S.A.

O. Bouhali⁷³, A. Celik, M. Dalchenko, M. De Mattia, A. Delgado, S. Dildick, R. Eusebi, J. Gilmore, T. Huang, T. Kamon⁷⁴, S. Luo, D. Marley, R. Mueller, D. Overton, L. Perniè, D. Rathjens, A. Safonov

Texas Tech University, Lubbock, U.S.A.

N. Akchurin, J. Damgov, F. De Guio, P.R. Duderov, S. Kunori, K. Lamichhane, S.W. Lee, T. Mengke, S. Muthumuni, T. Peltola, S. Undleeb, I. Volobouev, Z. Wang, A. Whitbeck

Vanderbilt University, Nashville, U.S.A.

B. Fabela Enriquez, S. Greene, A. Gurrola, R. Janjam, W. Johns, C. Maguire, A. Melo, H. Ni, K. Padeken, F. Romeo, P. Sheldon, S. Tuo, J. Velkovska, M. Verweij, Q. Xu

University of Virginia, Charlottesville, U.S.A.

M.W. Arenton, P. Barria, B. Cox, R. Hirosky, M. Joyce, A. Ledovskoy, H. Li, C. Neu, Y. Wang, E. Wolfe, F. Xia

Wayne State University, Detroit, U.S.A.

R. Harr, P.E. Karchin, N. Poudyal, J. Sturdy, P. Thapa, S. Zaleski

University of Wisconsin — Madison, Madison, WI, U.S.A.

J. Buchanan, C. Caillol, D. Carlsmith, S. Dasu, I. De Bruyn, L. Dodd, B. Gomber⁷⁵, M. Grothe, M. Herndon, A. Hervé, U. Hussain, P. Klabbbers, A. Lanaro, K. Long, R. Loveless, T. Ruggles, A. Savin, V. Sharma, N. Smith, W.H. Smith, N. Woods

†: Deceased

1: Also at Vienna University of Technology, Vienna, Austria

2: Also at IRFU, CEA, Université Paris-Saclay, Gif-sur-Yvette, France

3: Also at Universidade Estadual de Campinas, Campinas, Brazil

4: Also at Federal University of Rio Grande do Sul, Porto Alegre, Brazil

5: Also at Université Libre de Bruxelles, Bruxelles, Belgium

6: Also at University of Chinese Academy of Sciences, Beijing, China

7: Also at Institute for Theoretical and Experimental Physics named by A.I. Alikhanov of NRC ‘Kurchatov Institute’, Moscow, Russia

8: Also at Joint Institute for Nuclear Research, Dubna, Russia

9: Also at Suez University, Suez, Egypt

10: Now at British University in Egypt, Cairo, Egypt

11: Also at Zewail City of Science and Technology, Zewail, Egypt

12: Also at Department of Physics, King Abdulaziz University, Jeddah, Saudi Arabia

13: Also at Université de Haute Alsace, Mulhouse, France

14: Also at Skobeltsyn Institute of Nuclear Physics, Lomonosov Moscow State University, Moscow, Russia

15: Also at CERN, European Organization for Nuclear Research, Geneva, Switzerland

16: Also at RWTH Aachen University, III. Physikalisches Institut A, Aachen, Germany

17: Also at University of Hamburg, Hamburg, Germany

18: Also at Brandenburg University of Technology, Cottbus, Germany

19: Also at Institute of Physics, University of Debrecen, Debrecen, Hungary

20: Also at Institute of Nuclear Research ATOMKI, Debrecen, Hungary

- 21: Also at MTA-ELTE Lendület CMS Particle and Nuclear Physics Group, Eötvös Loránd University, Budapest, Hungary
- 22: Also at Indian Institute of Technology Bhubaneswar, Bhubaneswar, India
- 23: Also at Institute of Physics, Bhubaneswar, India
- 24: Also at Shoolini University, Solan, India
- 25: Also at University of Visva-Bharati, Santiniketan, India
- 26: Also at Isfahan University of Technology, Isfahan, Iran
- 27: Also at Plasma Physics Research Center, Science and Research Branch, Islamic Azad University, Tehran, Iran
- 28: Also at Italian National Agency for New Technologies, Energy and Sustainable Economic Development, Bologna, Italy
- 29: Also at Centro Siciliano di Fisica Nucleare e di Struttura della Materia, Catania, Italy
- 30: Also at Università degli Studi di Siena, Siena, Italy
- 31: Also at Scuola Normale e Sezione dell'INFN, Pisa, Italy
- 32: Also at Kyung Hee University, Department of Physics, Seoul, Korea
- 33: Also at Riga Technical University, Riga, Latvia
- 34: Also at International Islamic University of Malaysia, Kuala Lumpur, Malaysia
- 35: Also at Malaysian Nuclear Agency, MOSTI, Kajang, Malaysia
- 36: Also at Consejo Nacional de Ciencia y Tecnología, Mexico City, Mexico
- 37: Also at Warsaw University of Technology, Institute of Electronic Systems, Warsaw, Poland
- 38: Also at Institute for Nuclear Research, Moscow, Russia
- 39: Now at National Research Nuclear University 'Moscow Engineering Physics Institute' (MEPhI), Moscow, Russia
- 40: Also at St. Petersburg State Polytechnical University, St. Petersburg, Russia
- 41: Also at University of Florida, Gainesville, U.S.A.
- 42: Also at P.N. Lebedev Physical Institute, Moscow, Russia
- 43: Also at California Institute of Technology, Pasadena, U.S.A.
- 44: Also at Budker Institute of Nuclear Physics, Novosibirsk, Russia
- 45: Also at Faculty of Physics, University of Belgrade, Belgrade, Serbia
- 46: Also at University of Belgrade, Belgrade, Serbia
- 47: Also at INFN Sezione di Pavia^a, Università di Pavia^b, Pavia, Italy
- 48: Also at National and Kapodistrian University of Athens, Athens, Greece
- 49: Also at Universität Zürich, Zurich, Switzerland
- 50: Also at Stefan Meyer Institute for Subatomic Physics (SMI), Vienna, Austria
- 51: Also at Adiyaman University, Adiyaman, Turkey
- 52: Also at Beykent University, Istanbul, Turkey
- 53: Also at Istanbul Aydin University, Istanbul, Turkey
- 54: Also at Mersin University, Mersin, Turkey
- 55: Also at Piri Reis University, Istanbul, Turkey
- 56: Also at Gaziosmanpasa University, Tokat, Turkey
- 57: Also at Ozyegin University, Istanbul, Turkey
- 58: Also at Izmir Institute of Technology, Izmir, Turkey
- 59: Also at Marmara University, Istanbul, Turkey
- 60: Also at Kafkas University, Kars, Turkey
- 61: Also at Istanbul University, Istanbul, Turkey
- 62: Also at Istanbul Bilgi University, Istanbul, Turkey
- 63: Also at Hacettepe University, Ankara, Turkey
- 64: Also at Rutherford Appleton Laboratory, Didcot, United Kingdom

- 65: Also at School of Physics and Astronomy, University of Southampton, Southampton, United Kingdom
- 66: Also at Monash University, Faculty of Science, Clayton, Australia
- 67: Also at Bethel University, St. Paul, U.S.A.
- 68: Also at Karamanoğlu Mehmetbey University, Karaman, Turkey
- 69: Also at Purdue University, West Lafayette, U.S.A.
- 70: Also at Bingol University, Bingol, Turkey
- 71: Also at Sinop University, Sinop, Turkey
- 72: Also at Mimar Sinan University, Istanbul, Istanbul, Turkey
- 73: Also at Texas A&M University at Qatar, Doha, Qatar
- 74: Also at Kyungpook National University, Daegu, Korea
- 75: Also at University of Hyderabad, Hyderabad, India